

https://dspace.org/

The transmembrane region of CLIC1 is helical in membrane-mimetic solvents

Ngubane, Nomxolisi Chloe Mina-Liz

2012-06-13
http://hdl.handle.net/10539/11477

Downloaded from a DSpace repository. https://dspace.org/

THE TRANSMEMBRANE REGION OF CLIC1 IS HELICAL IN MEMBRANE-MIMETIC SOLVENTS

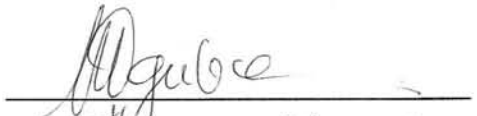
Nomxolisi Chloë Mina-Liz Ngubane

A dissertation submitted to the Faculty of Science, University of the Witwatersrand, Johannesburg, in fulfilment of the requirements for the degree of Master of Science.
Johannesburg, 2011

Declaration

I declare that this dissertation is my own, unaided work. It is being submitted for the degree of Master of Science in the University of the Witwatersrand, Johannesburg. It has not been submitted for any other degree or examination at any other University.

Nomxolisi Chloë Mina-Liz Ngubane



28th day of February, 2012

Abstract

CLIC1 is a member of the chloride intracellular channel proteins (CLICs), a group of amphitropic chloride channels. CLICs are able to transform from a cytoplasmic form to a membrane-bound form by a mechanism thought to involve a structural rearrangement, facilitated by movement to a low pH environment, that reveals the hydrophobic transmembrane region (TMR) in the N-domain. The TMR forms an alpha-helix-beta-strand structure in the soluble CLIC1 which is then thought to form the transmembrane helix in the membrane. The aim was to characterise the structure and stability of two peptides containing the TMR in membrane-mimetic solvents using far-UV circular dichroism and fluorescence. The first peptide, β1-TMR, corresponding to the first 52 amino acids of CLIC1 was to be purified from a fusion protein with GST, obtained from overexpression in bacterial culture. The second peptide, a synthetic 30 residue peptide corresponding to the sequence range Cys24-Val46 and referred to as the TMR peptide was commercially obtained. Overexpression and purification of the GST fusion protein as well as liberation of the β1-TMR from the fusion partner using thrombin was achieved but isolation of the β1-TMR peptide from GST proved unsuccessful. Sodium dodecyl sulphate (SDS) and 2,2,2-trifluoroethanol (TFE) were used as membrane mimetics to observe the structure of the TMR peptide. The secondary structure of the peptide increased with increasing TFE and SDS concentrations until 40% TFE where it was ~52% helical and 16 mM SDS where it was ~22% helical. pH had no effect on the secondary or tertiary structure of the peptide. Chemical and thermal denaturation of the TMR revealed that the helix formed in the membrane environment followed a non-cooperative unfolding pathway over a large temperature and denaturant range, indicating a very stable structure as would be required for a transmembrane helix. These results suggest that the TMR would form a stable transmembrane helix of CLIC1 in the hydrophobic environment of the membrane as a result structural elsewhere in the mature protein facilitate by a change in pH.

Acknowledgements

My sincere thanks goes out to my supervisors Prof. H.W. Dirr and Dr. S. Fanucchi for granting me this research opportunity and their continual support, guidance and patience throughout.

I would also like to extend my thanks to my colleagues in the Protein Structure Function Research Unit whose friendships and support contributed in different ways in and out of the lab.

In addition, I thank the National Research Foundation of South Africa and the University of the Witwatersrand for the financial support.

Table of contents

Abstract ii

Acknowledgements iii

List of Figures vi

List of Tables vii

Abbreviations viii

1. Introduction 1
    1.1. Transmembrane domains 1
    1.2. Chloride channels 2
    1.3. Amphitropic proteins 3
    1.4. Chloride intracellular channel (CLIC) proteins 5
    1.5. Transmembrane region of CLIC1 10
2. Objective 15
3. Experimental procedures 16
    3.1. Materials 16
    3.2. Production of β1-TMR 16
        3.2.1. Plasmid purification and verification 17
        3.2.2. GST-fusion protein overexpression and purification 17
        3.2.3. Off-column thrombin digestion of fusion protein 18
        3.2.4. Size-exclusion chromatography 19
    3.3. Acquisition of synthetic TMR peptide 20
    3.4. Solubilisation of TMR peptide 20
        3.4.1. Peptide concentration determination 21
    3.5. Characterisation of TMR peptide in membrane-mimetic systems 22
        3.5.1. Circular dichroism 22
        3.5.2. Fluorescence 23
            3.5.2.1. Steady-state fluorescence 23
            3.5.2.2. Acrylamide quenching 23
        3.5.3. Behaviour of TMR in SDS micelles 24
        3.5.4. Effect of environment of TMR peptide: pH and TFE studies 25
        3.5.5. Stability studies 25
4. Results 27

4.1. Purification of β1-TMR peptide 27
4.1.1. DNA sequencing 27
4.1.2. Protein expression and purification 28
4.2. Solubilisation of TMR peptide 31
4.3. Characterisation of the structure and stability of the TMR peptide 37
4.3.1. pH dependence 44
4.3.2. Stability 47
5. Discussion 49
5.1. Folding model of CLIC1 49
5.2. Structure of the TMR peptide 50
5.3. Effect of pH on secondary structure 52
5.4. Stability of the TMR peptide secondary structure 53
6. Conclusion 55
7. References 56

List of Figures

Figure 1: The transmembrane regions of amphitropic proteins 4
Figure 2: Structural alignment of CLIC1 with GST-O1-1 6
Figure 3: Crystal structure of soluble CLIC1 8
Figure 4: Hydrophobicity plot for CLIC1 11
Figure 5: TMpred output for CLIC1 12
Figure 6: Structure-based sequence alignment for the TM regions of CLIC proteins 12
Figure 7: Sequencing results of pGEX-CLIC1 plasmid 27
Figure 8: Expression and purification of GST-(β1-TMR) fusion protein 29
Figure 9: Thrombin digestion of the GST-(β1-TMR) fusion protein 30
Figure 10: Far-UV CD spectra of the TMR in aqueous buffer 32
Figure 11: The TMR peptide in ethanol 34
Figure 12: Far-UV CD spectra of the TMR peptide in methanol 35
Figure 13: Far-UV CD spectra of the TMR peptide in 50% TFE 36
Figure 14: Far-UV CD of the TMR peptide as a function of TFE concentration 38
Figure 15: Dichroweb analysis of the TMR peptide in 40% TFE 39
Figure 16: Effect of concentration on secondary structure of the TMR peptide in 40% TFE 40
Figure 17: Far-UV CD of the TMR peptide in SDS 42
Figure 18: Dichroweb analysis of the TMR peptide in 16mM SDS 43
Figure 19: Effect of pH on the secondary structure of the TMR peptide in 40% TFE 45
Figure 20: Acrylamide quenching of the TMR peptide in 50% TFE 46
Figure 21: Unfolding of the TMR peptide in 40% TFE 48

List of Tables

Table 1: Secondary structure composition of the TMR peptide in 40% TFE 39

Table 1: Secondary structure composition of the TMR peptide in 16mM SDS 43

Abbreviations

α	alpha
β	beta
2YT	two times yeast extract and tryptone media
A_{280}	Absorbance at 280 nm
Å	Ångström
Ac	acetylation
Am	amidation
β1-TMR	peptide encompassing first 52 amino acids of CLIC1
CD	circular dichroism
CFTR	cystic fibrosis transmembrane regulator
CLC	chloride channels
CLIC	chloride intracellular ion channels
CMC	critical micellar concentration
Da	dalton
dH2O	distilled water
DNA	deoxyribonucleic acid
DTT	dithiothreitol
ε	molar extinction coefficient; dielectric constant
ExPasy	Expert Protein Analysis System
E222	ellipticity at 222 nm
EDTA	ethylediaminetetra-acetic acid
ER	endoplasmic reticulum
F_0	fluorescence intensity in the absence of quencher
F	fluorescence intensity in the presence of quencher
F355	fluorescence emission intensity at 355 nm
Far-UV CD	far-ultraviolet circular dichroism
ΔG	the change in Gibbs free energy
GABA	gamma-aminobutyric acid
GSH	glutathione
GRAVY	grand average of hydropathicity
GST	glutathione S-transferase
H^+	proton

HCl	hydrochloric acid
IPTG	isopropyl-1-thio-β-D-galactopyranoside
K_{SV}	Stern-Volmer quenching constant
LB	Luria-Bertani
λ_{max}	fluorescence emission wavelength maximum
M	molar
MAP	mitogen-activated protein
μM	micromolar
mM	millimolar
mdeg	millidegree
MRE	mean residue ellipticity
NATA	N-acetyl-tryptophanamide
nm	nanometers
NMR	nuclear magnetic resonance
NRMSD	normalised root mean square distance
OD	optical density
O-state	organic solvent-induced state
PAGE	polyacrylamide gel electrophoresis
PDB	Protein Data Bank
PFT	pore-forming toxin
rpm	revolutions per minute
RyR	ryanodine receptor
SDS	sodium dodecyl phosphate
SEC	size exclusion chromatography
*Sj*GST	*Schistosoma japonicum* glutathione S-transferase
SOC	Super optimal broth with Catabolic repressor
STE	sodium/tris/EDTA
TFE	2,2,2-trifluoroethanol
TM	transmembrane
TMR	peptide encompassing G22-R51 of CLIC1
Tris	Trizma base
UV	ultraviolet
YT	yeast tryptone

Standard one- and three-letter amino acid codes have been used throughout.

1. INTRODUCTION

1.1. Transmembrane domains

Biological membranes are made up of a variety of biological molecules, primarily lipids and proteins. The lipid component of membranes is composed of a range of amphipathic lipids made up of hydrophobic hydrocarbon tails and polar heads. The hydrophobic tails associate via hydrophobic interaction to form a lipid bilayer that has a hydrophobic core (Quinn, 1976; Tanford, 1980). The polar heads of the lipids are exposed to the aqueous surroundings and form the membrane surface with a net negative charge that attracts protons (H^+), and lowers the pH in this region to ~5.5 (Luckey, 2008; van de Goot *et al.*, 1991). The lipid bilayer allows for the diffusion of hydrophobic molecules but prevents the passage of polar solutes and charged molecules. The movement of such molecules is thus controlled by globular proteins that are embedded in the membrane, referred to as transmembrane or integral membrane proteins (Singer and Nicholson, 1972). These membrane proteins transport inorganic ions of appropriate size and charge through facilitated diffusion across an electrochemical or concentration gradient (Alberts *et al.*, 2002). They have membrane-spanning domains that anchor them within the membrane referred to as transmembrane (TM) domains. The TM domains of membrane proteins fold independently from the rest of the protein and are thermodynamically stable (Popot and Engelman, 1990). TM domains are usually single or multiple alpha-helical structures but can also be beta-barrel type structures as observed in bacterial proteins (Lee, 2005). These highly hydrogen bonded secondary structures lower the energy cost of transferring polar peptide bonds to a non-polar environment (Lee, 2005; Roseman, 1988). Helical TM domains are usually about 20 amino acids long, sufficient in length to span the membrane (White and Whimley, 1999). The central part of the transmembrane segment housed within the hydrophobic interior of the membrane is predominantly made up of apolar residues (Ala, Ile, Leu,Val, Phe) and as a result has a large hydrophobic surface (Arkin *et al.*, 1998; Landolt-Marticorena *et al.*, 1993). TM domains often contain charged residues (Arg, Asp, Glu, Lys) that are located at the membrane interface, which form strong stabilising interactions with the negatively charged lipid head groups and help to anchor the membrane protein in place (Hunte, 2005; von Heijne, 2006). Negatively charged residues that exist inside the bilayer are neutralised by the low pH at the membrane surface to allow them to enter the hydrophobic core (Flewelling and Hubbel, 1986; Krishtalik and Cramer, 1995). Aromatic residues comprised of both polar and apolar

moieties (Trp, Tyr, His) are often located at the boundary between the lipid headgroups and the hydrophobic core. The non-polar regions of these residues are often embedded in the hydrocarbon plane whilst the polar amide or hydroxyl groups protrude into the aqueous region, interacting with the lipid headgroups at the membrane interface (Ulmschneider *et al*., 2005; von Heijne, 2006; Yau *et al*., 1998). Trytophan is uniquely suited to interacting at the polar interface because of its significant dipole moment and its ability to act as a hydrogen bond donor, anchoring the helices within the membrane and modulating their interaction with the lipid bilayer (Jacobs and White, 1989; Landolt-Maricorena *et al.*, 1993; Tilley and Saibil, 2006; Ulmschneider and Sansom, 2001). This preference for aromatic residues at the membrane boundary is more pronounced in single-spanning membrane protein helices (Landolt-Marticorena, 1993). The presence of both charged and aromatic residues at the interface combines electrostatic and hydrophobic interactions to stabilise membrane proteins (Ulmschneider *et al.*, 2005).

1.2. Chloride channels

Ion channels are integral membrane proteins that form pores in membranes, allowing for the passage of ions into and out of the cell and may open in response to certain stimuli or cellular conditions (Jentsch *et al.*, 1994, Jentsch *et al.*, 2002). Chloride ions are the most physiologically abundant and predominantly conducted ion species (Jentsch *et al.*, 2002).

Chloride channels are a diverse group of channel proteins that regulate fundamental cellular processes (Jentsch *et al.*, 1994). They conduct chloride ions and occasionally other anions and contain between 1 and 12 transmembrane segments (Reviewed by Suzuki *et al.*, 2006). Chloride channels can be classified into four types: ligand-gated chloride channels such as the gamma-aminobutyric acid receptors (GABAs) and the glycine receptors which are activated by the binding of a ligand to the extracellular domain of the channel, the cystic fibrosis transmembrane conductance regulators (CFTRs), the voltage-dependent chloride ion channels (CLCs) and the chloride intracellular channels (CLICs) (Reviewed by Cromer *et al.*, 2002; Jentsch *et al.*, 2002). A distinguishing feature of the recently discovered CLIC proteins is their ability to exist in a soluble globular form as well as a membrane-bound form. They are thus termed amphitropic proteins.

1.3. Amphitropic proteins

Most integral membrane proteins are synthesised at the ribosome with an N-terminal signal peptide that directs their insertion into the membrane as they are translated (Borel and Simon, 1996; Do *et al.*, 1996). However, a small number of proteins are able to exist in a stable water-soluble form in the cytoplasm as well as an integral membrane-bound form. These are amphitropic proteins and they lack the aforementioned signal peptide and instead are translated into a soluble cytoplasmic form that later inserts into the membrane as a result of a trigger such as a change in pH or membrane lipid composition, oxidation, phosphorylation or ligand-binding (Reviewed by Cromer *et al.*, 2002 and Parker and Feil, 2005). This transition requires a dramatic reorganisation of the protein's structure but the details of the mechanism of membrane insertion remain unclear. The CLICs share their unusual structural duality and membrane autoinsertion with these proteins and are thought to insert into the membrane in a similar manner thus distinguishing them from other chloride channels. Members of this unusual group of proteins include bacterial toxins and mammalian proteins from the annexin and Bcl-2 families (as reviewed by Singh, 2010)

The pore-forming toxins (PFTs) are a group of toxic bacterial proteins that form large pores in the cell membranes of their target organisms, resulting in cell death. PFTs contain domains that enable their transition from the soluble to the membrane-bound state. These include a translocation and a channel forming domain (Reviewed by Parker and Feil, 2005). There are two groups of PFTs which are classified according to the distinct structures that make up their transmembrane domains.

The alpha-PFTs include colicin A, diphtheria toxin and Cry1. Colicin A unfolds a helical cluster in the C-domain to reveal a long, hydrophobic helical loop which drives membrane insertion and forms the transmembrane domain (Figure 1A) (Parker *et al.*, 1992). This process is dependent on the low pH at the membrane surface (Muga *et al.*, 1992) which allows colicin A to form a molten globule intermediate (Van der Goot *et al.*, 1991), effectively reducing the energy barrier required for unmasking the hydrophobic hairpin and facilitating membrane insertion by making the exchange of protein-protein interactions for protein-lipid interactions more energetically favourable (Lesieur *et al.*, 1997). The low pH also neutralises the acidic side chains of amino acids in the hairpin, rendering the face more hydrophobic and lowering the energy cost of inserting the helical hairpin into the membrane (Krishralik and Cramer, 1995). The pore-forming mechanism of some alpha-PFTs such as

diphtheria toxin further includes dimerisation to form the complete pore (Figure 1B) (Bennet *et al.*, 1994; Choe *et al.*, 1991)

The group of beta- PFTs includes δ-endotoxin, aerolysin, anthrax and perfringolysin, proteins whose transmembrane regions are made up of beta-strands. Alpha-haemolysin is a beta-PFT made up of 7 alpha-haemolysin units which contain a large number of beta-strands that assemble into a beta-barrel to form the transmembrane domain (Figure 1C) (Reviewed by Cromer *et al.*, 2002 and Guouax, 1998).

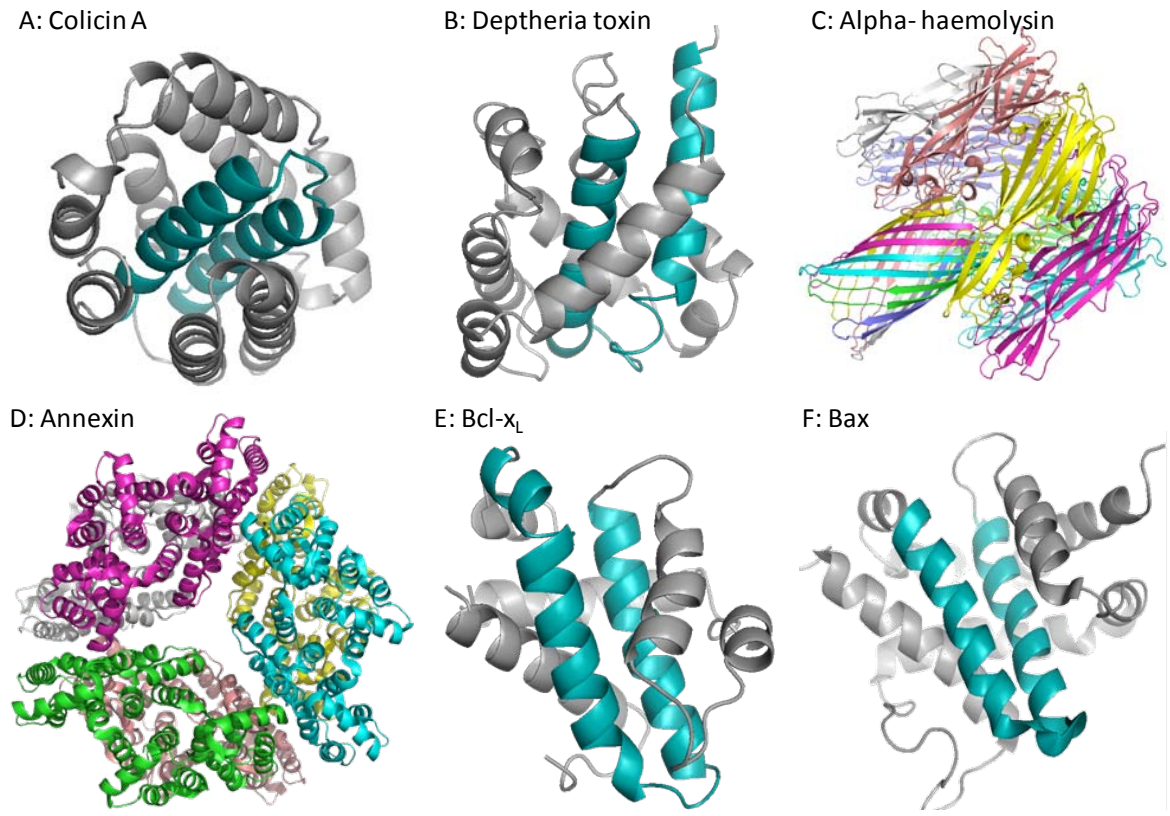


Figure 1: The transmembrane regions of amphitropic proteins
Ribbon representations of some amphitropic proteins. Helices highlighted in blue are the transmembrane helices. (**A**) Colicin A has a hydrophobic hairpin that inserts into the membrane; pdb file 1COL (Parker *et al.*, 1992). (**B**) A similar helix is observed in diphtheria toxin; pdb file 1DDT (Bennet *et al.*, 1994). (**C**). Alpha-hemolysin is a heptamer of subunits whose tails assemble into a beta-barrel that form the transmembrane region; pdb file 7HAL (Song *et al.*, 1996). (**D**) Annexin forms a hexamer before binding to the membrane; pdb file 1DM5 (Cartailler *et al.*, 2000). (**E**) Bcl-x$_L$; pdb file 1MAZ (Muchmore *et al.*, 1996) and (**F**) Bax; pdb file 1F16 (Suzuki *et al.*, 2000), have a helical loop that forms their TM. This figure was generated using PyMol™ v. 0.99 (DeLano Scientific, 2006).

Some mammalian proteins also display the amphitropic properties seen in the bacterial toxins. Annexins are a family of calcium-binding proteins that are involved in ion channel activity (Cartailler *et al.*, 2000). The naming member of this group, Annexin, does not enter the membrane but interacts with the negatively charged heads of the phospholipids in the bilayer after a hexamerisation step that is mediated by the binding of calcium to the C-terminal core region of the protein (Figure 1D) (Luecke *et al.*, 1995). Bcl-x_L is a member of the Bcl-2 family of apoptotic proteins regulating programmed cell death or apoptosis. Bcl-x_L inserts into the membrane by a pH dependent process (Schendel *et al.*, 1997) without forming a molten globule intermediate (Thuduppathy and Hill, 2006). Bcl-x_L is understood to convert into a membrane bound form by a 3-state process that involves it being anchored to the membrane by its C-domain before the insertion of a hydrophobic helical loop into the membrane (Figure 1E) (Thuduppathy *et al.*, 2006). Bax, another member of the Bcl-2 family, is thought to form an intermediate state that is bound to the membrane surface before oligomerising to form the functional pore (Figure 1F) (Garcia-Sáez *et al.*, 2004).

1.4. Chloride intracellular ion channel (CLIC) proteins

The CLIC proteins are a class of intracellular chloride channels that do not resemble other well-characterised chloride channel proteins. They do not share any structural or sequence homology with the other chloride channels (Reviewed in Cromer *et al.*, 2002 and Singh, 2010) and thus do not contain the characterised domains and sequences for ion selectivity and conductance (Dutzler *et al.*, 2001). The presence of only one putative transmembrane domain has also cast doubt on their ability to function as ion channels (Jentsch *et al.*, 2002). Furthermore, while other chloride channels localise to the plasma membrane, the CLIC proteins localise to the membranes of various intracellular organelles including the nucleus (Valenzuela *et al.*, 1997), mitochondria (Fernandez-Sales *et al.*, 1999), golgi vesicles (Edwards, 1999) and endoplasmic reticulum (ER) (Duncan *et al.*, 1997), in addition to the plasma membrane. The CLIC proteins have been shown to facilitate ion transport without additional subunits or accessory proteins (Chuang *et al.*, 1999; Littler *et al.*, 2005). Despite the evidence that the CLIC proteins can form functional chloride channels (Reviewed by Ashley 2003; Berryman *et al.*, 2004; Harrop *et al.*, 2001; Littler *et al.*, 2005; Tonini *et al.*, 2000), the lack of characteristic sequences and structures for ion conductance and selectivity has led to CLIC proteins being considered non-selective multi-ion pores rather than chloride-specific channels (Singh and Ashley, 2006).

Incidentally, the CLIC proteins share structural and low sequence homology (~15%) with members of the Omega glutathione transferase (Omega- GSTs) superfamily (reviewed by Cromer *et al.*, 2002; Harrop *et al.*, 2001; reviewed by Littler *et al.*, 2010). These are a group of soluble homodimeric proteins with a thioredoxin fold in the N-domain and an all-helical C-domain (Figure 2). The thioredoxin fold is also present in a number of other proteins (SCOP: Murzin *et al.*, 1995), although they have very little sequence similarity and have unrelated roles (Martin, 1995).

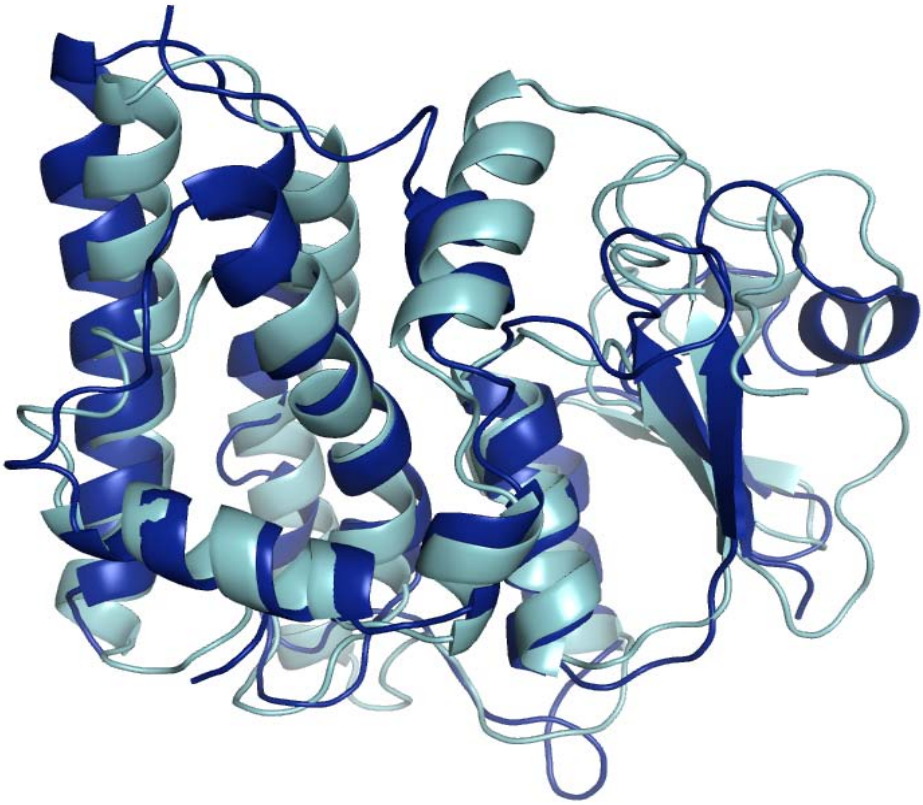


Figure 2: Structural alignment of CLIC1 with GST O1-1.
CLIC1 (dark blue) alignment with GST O1-1 (light blue), with RMSD = 1.65 Å. The alignment was performed using the MultiProt server (http://bioinfo3d.cs.tau.ac.il/MultiProt/) (Shatsky et al., 2004) and PDB codes 1K0N (Harrop *et al*., 2001) and 1EEM (Board *et al*., 2000). Image generated using PyMOL™ v. 0.99 (DeLano Scientific, 2006).

The CLIC proteins are widely distributed in tissues and organisms (Berry *et al.*, 2003) and have 7 human homologues (Reviewed by Ashley, 2003, Cromer *et al.*, 2002 and Littler *et al.*, 2010) and orthologues in invertebrate species such as *Caenorhabditis elegans* (Berry *et al.*,, 2003), *Drosophila melanogaster* (Shorning *et al.*, 2003) and some plants including *Arabidopsis thaliana* (Elter *et al.*, 2007). The human CLIC proteins share a 238 amino acid CLIC module in the C-domain with variation in the length of the remaining sequence

between the different proteins (Berry *et al.*, 2003; Nishizawa *et al.*, 2000) and show up to 67% sequence identity (Berryman *et al.*, 2004).

Invertebrate CLIC proteins have a lower sequence identity to the human CLIC proteins (Berry *et al.*, 2003) and lack some of the conserved N-domain residues; they also lack the glutathione (GSH) binding site (Cys24 in CLIC1) observed in the human CLIC proteins (Harrop *et al.*, 2001) and instead have a divalent metal ion binding site (Berry and Hobert, 2006; Littler *et al.*, 2003). In addition, the invertebrate CLICs contain an extension in the C-domain (Littler *et al.*, 2003). The CLIC proteins are said to have evolved separately from each other, but this divergence in sequence does not affect their overall structure which is important for their function (Berry and Hobert, 2006) and the conservation of this structure implies an important physiological role. The CLICs have been implicated to play a role in a variety of important cellular processes including apoptosis (Fenandez-Sales *et al.*, 2002), cell division, cell cycle regulation (Tonini *et al.*, 2000; Valenzuela *et al.*, 2000) as well as signal transduction and intracellular transport (Berryman and Bretscher, 2000), by controlling cellular chloride concentrations (Reviewed by Debska, 2001). Despite this, their exact function remains unknown.

CLIC1 is a protein of 241 amino acids (26.9 kDa) shown to localise to and associate with both the nuclear and plasma membranes and function as an ion channel with selectivity for anions (Harrop *et al.*, 2001; Singh and Ashley, 2007; Valenzuela *et al.*, 1997). The crystal structure of soluble CLIC1 (Harrop *et al.*, 2001) shows a monomeric protein with a thioredoxin-like fold in the N-domain. The N-domain includes a catalytic cysteine-24 residue that allows it to covalently bind the GST substrate glutathione (GSH) by means of a mixed disulfide bond. CLIC1 has an all-helical C-domain (Figure 3), resulting in an overall structure very much like that of Omega-GST (Harrop *et al.*, 2001). CLIC1 is mostly alpha-helical with only ~ 8% of beta-strand content in its reduced monomeric state. It was proposed that because of the small size of CLIC1, it is likely that it can oligomerise to form fully functional channels (Singh and Ashley, 2006; Warton *et al.*, 2002). Under oxidising conditions, CLIC1 undergoes a structural transition that is mediated by the formation of an intramolecular disulphide bond between cysteines 24 and 59 (Littler *et al.*, 2004). This results in a major structural rearrangement leading to an all-helical N-domain and the exposure of a large hydrophobic surface that is stabilised *in vitro* by a reversible transition into a dimer (Littler *et al.*, 2004). *In vivo*, this hydrophobic surface is thought to represent the membrane-docking

surface of CLIC1. The oxidised dimeric form maintains the ability to form chloride channels in artificial bilayers and micelles and both cysteines (Cys24 and Cys59) are required for channel activity (Littler *et al.*, 2004).

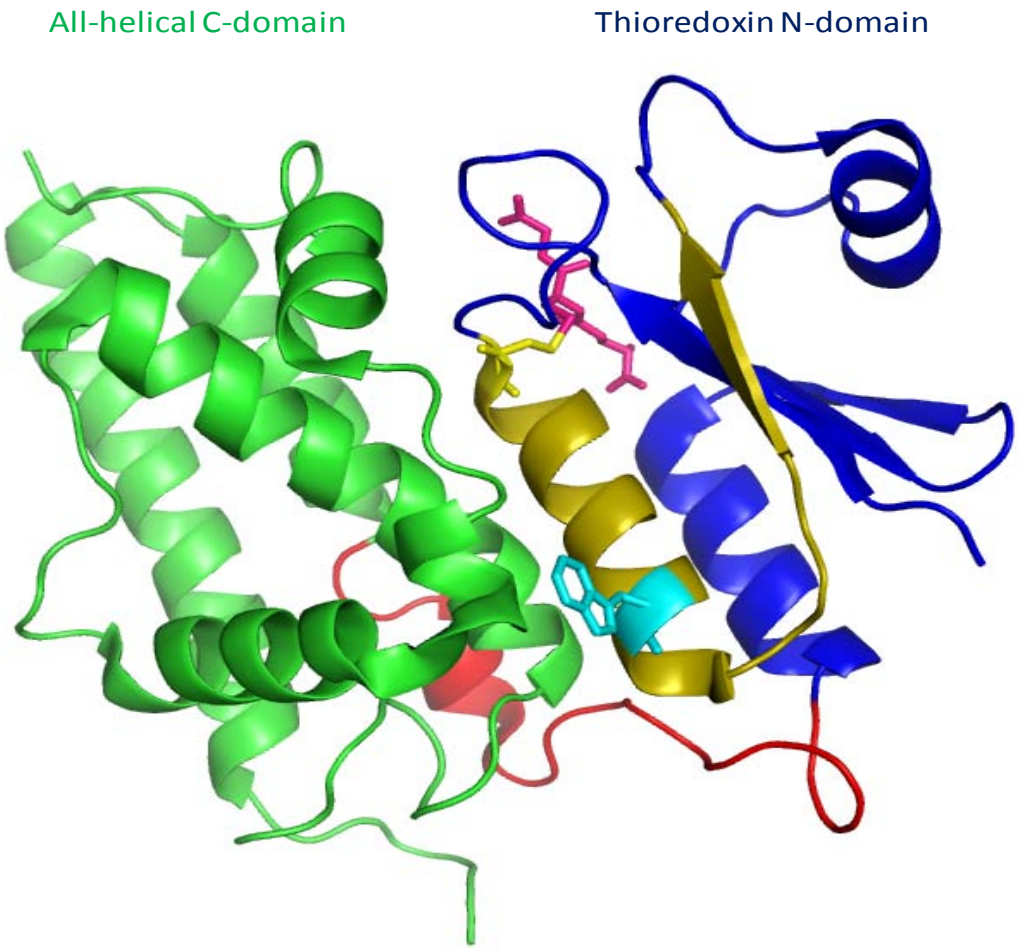


Figure 3: Crystal structure of soluble CLIC1
A ribbon representation of the crystal structure of soluble CLIC1. The thioredoxin N-domain (blue) contains the active site with the catalytic Cys24 (yellow) bound to glutathione (pink) as well as the transmembrane region (gold) with Trp35 (cyan). The C-domain (green) is all-helical and the two domains are joined by a proline-rich loop (red). This figure was generated using PyMol v0.99 (DeLano Scientific, 2006) and the CLIC1 pdb file 1K0N (Harrop *et al.*, 2001).

CLIC2 is a 243 residue protein that shares over 58% sequence identity with CLIC1, differing mainly by a loop region between helices 5 and 6 (Board *et al.*, 2004). CLIC2 was found to have little catalytic activity with typical glutathione transferase substrates and to be a strong inhibitor of cardiac ryanodine receptor (RyR) channels and is therefore thought to play a role in the maintenance of intracellular calcium homeostasis (Board *et al.*, 2004; Dulhunty, 2001).

CLIC3 is a 207 residue protein that localises to the nucleus and has been shown to associate with MAP kinase (Qian *et al.,* 1999). It shares the lowest sequence identity with CLIC1 (49 %) and has a relatively narrow hydrophobic domain that might rule out a direct role in channel formation. It has been proposed that CLIC3 modulates chloride conductance at the nuclear membrane and activates the MAP kinase signal transduction pathway implying a role in cell growth (Qian *et al.,* 1999).

CLIC4 has been shown to associate with lipid bilayers and induce the efflux of chloride ions from artificial liposomes in a concentration-dependent manner at low pH (Littler *et al.,* 2005). CLIC4 shares 67% sequence identity with CLIC1 and this is evident in its crystal structure (Littler *et al.,* 2005) showing a GST-like structure which is highly homologous to that of CLIC1. Unlike CLIC1, CLIC4 does not form dimers under oxidising conditions (Littler *et al.,* 2004). This is because CLIC4 does not contain the cysteine residue at position 59 observed in CLIC1, which would mediate the formation of an intramolecular disulphide bond that would stabilise a dimeric form. The crystal structure of a trimeric CLIC4 has been described by Li and co-workers (2006), which may represent a unique mechanism of assembly for the oligomerisation of CLIC4 without the formation of an intramolecular disulfide bond.

CLIC5B is the human homologue of the bovine CLIC protein, p64 and a splice variant of CLIC5A (Shanks *et al.,* 2002). It is a 410 amino acid protein, of which 238 residues in the C-domain are identical to that of CLIC5A. CLIC5A has been shown to be a component of a cytoskeletal complex (Berryman and Bretscher, 2000) and to function as a chloride channel (Berryman *et al.,* 2004). CLIC5B has not yet been shown to function as a chloride channel.

CLIC6 is a 627 residue human homologue of the rabbit CLIC parchorin (Freidli *et al.,* 2003) that has been shown to move from the cytoplasm to the plasma membrane when chloride levels are low (Nishizawa *et al.,* 2000) but has not been demonstrated to function as a chloride channel as yet.

1.5. Transmembrane region of CLIC1

Initially, the CLIC proteins' similarities to alpha-PFTs lead researchers to propose that the CLIC proteins might use a similar mechanism for membrane insertion (Tulk *at al.,* 2002). Alpha- PFTs unfold to expose a long hydrophobic helical loop that translocates the proteins into the membrane and forms the transmembrane helix as a result of a change in pH (Parker

et al., 1989; reviewed in Cromer, 2002). The CLIC proteins contain a similar helix, h6 in their C-domain. Indeed, hydrophobicity plots (Kyte and Doolittle, 1982) show that this region has significant hydrophobicity with the potential to insert into the membrane, but the plots also show that another region, near the N-domain (h1&s2) also exhibits sizable hydrophobicity (Figure 4). Subsequent studies using FLAG epitopes (Tonini *et al.*, 2000), terminal-directed antibodies (Proustki *et al.*, 2002) and proteinase K digestion (Duncan *et al.*, 1997) of the membrane inserted form showed that in the membrane-inserted CLIC1, the C-domain locates to the cytoplasm while the N-terminal is inserted into the membrane with Cys-24 localising to the exterior of the membrane. Analysis of the CLIC1 amino acid sequence using TMpred (Hofmann and Stoffel, 1993), an algorithm that predicts transmembrane helices, indicates that residues 21 to 46 in the N-domain of CLIC1 are most likely to form the transmembrane region (TMR), with the rest of the N-terminal locating to the outside of the membrane (Figure 5). It was thus proposed that the TMR was a 23 residue fragment located in the N-domain between the residues Cys24-Val46 in CLIC1 (Berry and Hobert, 2003), a region that is highly conserved in the CLIC proteins (Figure 6). This sequence is arranged with charged residues flanking a 10 residue non-polar sequence, a typical arrangement for a transmembrane region (Sakai and Tsukihara, 1998). In the soluble form, this region forms an alpha-helix (h1) and beta-strand (s2) structure (already shown in Figure 3) and according to AGADIR, a tool used to predict the helical behaviour of peptides (Muňoz and Serrano, 1997; Lacroix *et al.* 1998), this region has a high propensity to form a helix. This region is long enough to span the membrane (31Å) and does not contain acidic residues, an essential feature for an anion channel. The TMR is consistently aliphatic amongst all CLIC proteins (Berry and Hobert, 2003) but the charged molecules are not highly conserved (Figure 6) and this has been postulated to lead to non-specific ion pores (Berry and Hobert 2006; Sakai and Tsukihara, 1998).

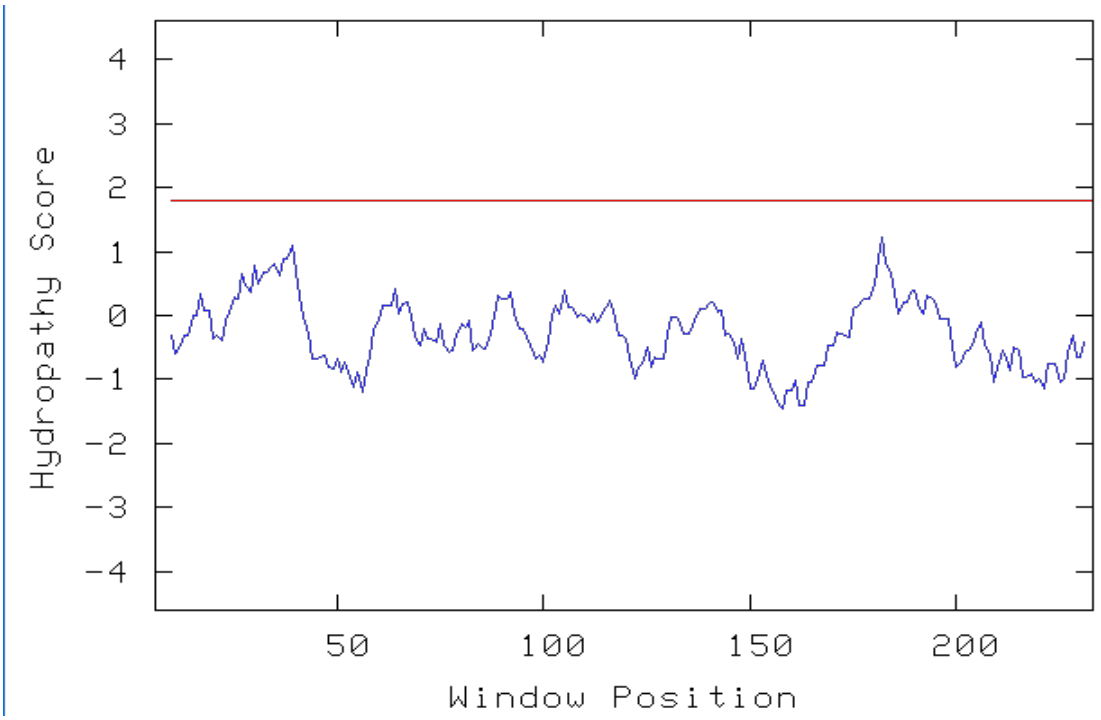


Figure 4: Hydrophobicity plot for CLIC1

This shows two areas in the CLIC1 protein sequences that have significant hydrophobicity and thus the potential to form a transmembrane helix. These regions are in the vicinity of the described N-domain TMR (h1 and s2) and h6 in the C-domain. This image was constructed using the Kyte-Doolittle plot using the parameters described in Kyte and Doolittle (1982) with a window size of 19 to predict hydrophobic regions that could form a transmembrane region. Generally the hydropathy score has to be above 1.6 to indicate possible transmembrane regions, but the hydropathy scores of the two regions above are distinct from the rest of the protein and can thus be considered when searching for the transmembrane region of CLIC1.

Studies conducted on this TMR show that this region is necessary for both membrane localisation and ion channel function. Berry and Hobert (2003 and 2004) used the first 66 amino acids to study the TMR of the *Caernorhabditis elegans* CLIC protein, EXC-4. They truncated helix 6 (h6) from the C-domain and this did not affect membrane insertion but the deletion of the 66 amino acid N-terminal sequence resulted in the failure of EXC-4 to localise to the membrane. The deletion of the beta-strand (s2) resulted in incomplete membrane insertion and a mutation of the Leu46 residue in h1 to a proline disrupted membrane insertion. An additional helix (h1) added to the N-terminal of the protein did not disrupt membrane insertion.

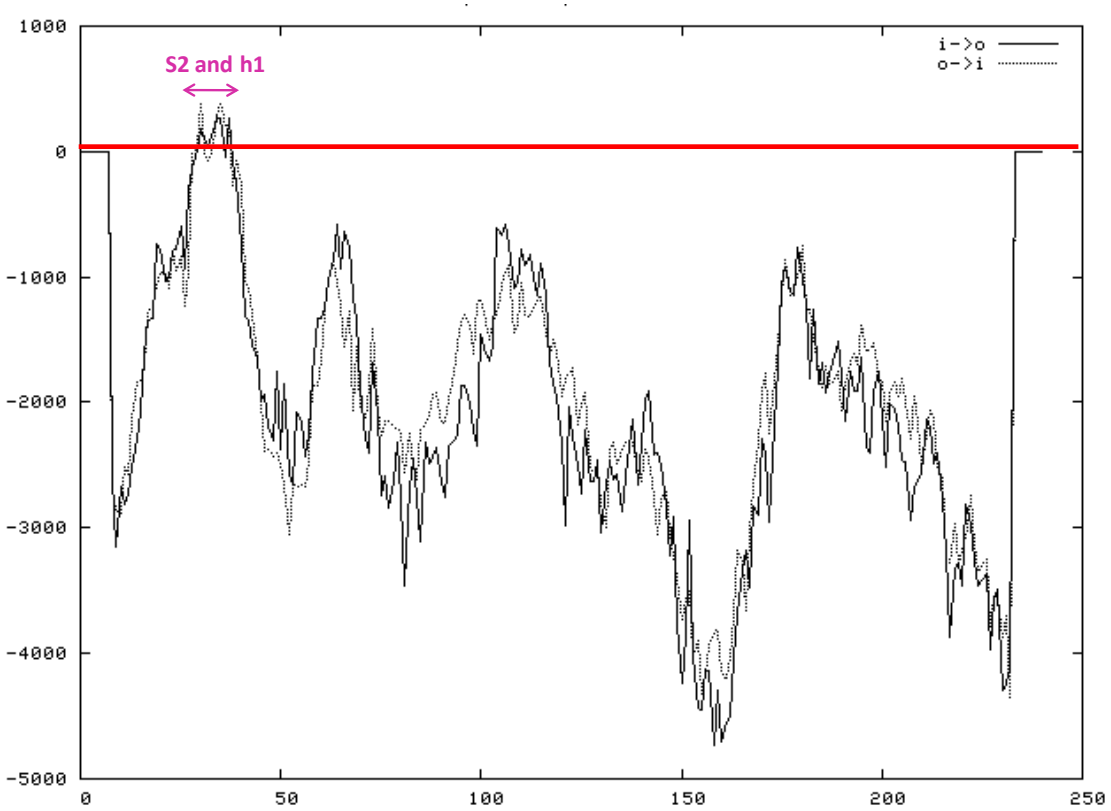


Figure 5: TMpred output for CLIC1

This shows results for two orientations: the N-terminal region locating to the outside (dotted) and the inside (solid) of the membrane. Both plots indicate that the TMR helix is located in the N-domain between residues 21-46 but the orientation with the N-terminal region locating outside the cell, has a higher score (394 in comparison to 278) when the N-terminal regionis inside the cell, indicating that this is the preferred orientation with Leu36 at the center of the TM helix. This figure was generated using the online tool TMpred (Hofmann and Stoffel, 1993)



Figure 6: Structure-based sequence alignment of the TM regions of CLIC proteins

The region in bold is the TMR. This 23 residue region is highly conserved in all the CLIC structures. The 18 residue sequence preceding the TMR is also highly conserved. This alignment was obtained using Vast (Madej *et al.*, 1995) with the PDB files 1K0M (CLIC1) (Harrop *et al.*, 2001), 2PER (CLIC2) (Mi *et al.*, 2008), 3FY7 (CLIC3) (Littler *et al.*, 2009), 2AHE (CLIC4) (Littler *et al.*, 2005), 2YV7 (exc-4) and 2YV9 (DmCLIC) (Littler *et al.*, 2008).

They concluded that h6 did not have role in membrane localisation, that the N-terminal sequence was fundamental to membrane insertion and function and that its conserved secondary structure was necessary and sufficient for membrane insertion while the rest of the N-terminal sequence (up to Cys24) was not necessary for but did not hinder membrane insertion, hence the extended N-terminal regions in other CLIC proteins such as CLIC5B and CLIC6. Duncan and co-workers (1997) also demonstrated that this 6 kDa N-terminal fragment formed a single transmembrane region in CLIC4 by treating CLIC4-microsomes with proteinase K.

Singh and Ashley (2007) characterised the TMR for CLIC4 using the first 61 amino acids. The TMR was able to form ion channels although the conductance was reduced and ion selectivity was absent, they concluded that the 61 amino acid sequence contained the transmembrane region of CLIC4 and suggested that the C-domain confers ion selectivity. This was further confirmation that the transmembrane region of CLIC proteins is located in the N-domain. When the CLIC1 sequence is aligned with the TMRs that have already been characterised in CLIC4 and EXC-4, the TMRs align with the first 52 amino acids of CLIC1 (Figure 6) which form a $\beta1\alpha1\beta2$ supersecondary motif in the soluble structure.

To form the transmembrane structure, the N-domain must detach from the C-domain of soluble CLIC1, extend and refold to expose buried hydrophobic residues and allow the replacement of protein-protein interactions with protein-lipid interactions as it penetrates the lipid bilayer. pH has been cited as a critical factor in this transition, after observations that channel formation and activity increased with a change from neutral to a more acidic pH (Cromer *et al.*, 2007; Goodchild *et al.*, 2009; Littler *et al.*, 2004; Littler *et al.*, 2008; Tulk *et al.*, 2002; Warton *et al.*, 2002). The low stability and enhanced flexibility of the N-domain observed at low pH (Fanucchi *et al.*, 2008; Stoychev *et al.*, 2009), makes it more probable that it would undergo the structural reorganisation required to insert into the membrane. The TMR is thought to be destabilised as it approaches the membrane and enters a lower pH environment, before independently extending and refolding into a helical structure that can insert into the membrane (Fanucchi *et al.*, 2008). Changes in the soluble CLIC1 structure where the N-domain undergoes a structural transition into an all-helical form at low pH have been postulated to form part of the transition into a membrane-bound CLIC1 (Reviewed by Singh, 2010).

2. OBJECTIVE

Despite all the evidence regarding the location of the TMR of CLIC and the models that have been proposed as to how this region comes to be in the membrane, not much is known about its exact structure within the membrane. Researchers have postulated that in the membrane, this region forms a transmembrane helix that then interacts with other transmembrane helices to form a higher order structure (Littler *et al.*, 2004; Singh and Ashley, 2006; 2007; reviewed by Singh, 2010; Warton *et al.*, 2002). In order to better understand the mechanisms by which the CLIC proteins insert into the membrane, we need to elucidate the structure of the TMR region which facilitates their membrane insertion and subsequently their function as ion channels. The primary objective of this work was to characterise the structure and stability of the TMR of CLIC1 in membrane-mimetic systems.

AIMS:

1. To generate two peptides containing the TMR of CLIC1
    - Use recombinant protein overexpression to produce and purify **β1-TMR –** the first 52 amino acids of CLIC1 containing β1 and the TMR
    - Design and commercially obtain chemically synthesised **TMR** – a 30-mer peptide encompassing residues Gly22 to Arg51

2. To characterise the structure of the peptides in membrane mimetic solvents
3. To study the effect of pH on the structure
4. To characterise the stability of the structure

3. EXPERIMENTAL PROCEDURES

3.1. Materials

The pGEX-4T-1 vector containing cDNA to encode wild-type GST- CLIC1 fusion protein with a stop codon incorporated at position 193 to produce the GST-(β1-TMR) fusion protein was a obtained from Dr. S. Fanucchi, Protein Structure Function Research Unit, University of the Witwatersrand, Johannesburg. *Escherichia coli* BL21(DE3) pLysS competent cells were obtained from Stratagene (USA). Dithiothreitol (DTT), reduced glutathione (GSH), human plasma thrombin (T6884), GSH-agarose, SDS-PAGE low molecular weight markers and 2,2,2-trifluoroethanol were purchased from Sigma-Aldrich (USA). Ultrapure urea was purchased from Merck (South Africa). The SDS-PAGE molecular weight marker (#SM0431), isopropyl-1-thio-β-D-galactopyranoside (IPTG) and GeneJet Kit for plasmid DNA purification were purchased from Fermentas (USA). All other chemicals were of analytical grade.

3.2. Production of β1-TMR

Competent *Escherichia coli* BL21(DE3) pLysS cells were transformed with the pGEX-4T-1 plasmid containing the CLIC1 cDNA using the transformation protocol as first described by Cohen and co-workers (1974). *Escherichia coli* BL21(DE3) pLysS cells are able to take up DNA. They are able to grow in minimal medium and are deficient in key proteases that would degrade abnormal and/or extracellular protein before and after lysis (Lim *et al.*, 1946; Wood, 1966). They also provide for a good expression system because they contain a T7 promoter that is capable of producing large amounts of protein (Studier and Moffatt, 1987). The pGEX-4T-1 vector encodes a GST from *Schistosoma japonicum* as part of a fusion protein with the target protein and contains a thrombin cleavage site located between the *Sj*GST and CLIC1 sequences allowing for on- or off-column cleavage of the target protein from the GST with thrombin. Competent *Escherichia coli* BL21 (DE3) pLysS cells were thawed on ice for 10 minutes, plasmid DNA was added and the mixture was stored on ice for a further 30 minutes. The mixture was then heat-shocked at 42 °C for 60 seconds and immediately transferred back to ice for 2 minutes. Super optimal broth with Catabolic repressor (SOC medium) was added to the reaction mixture which was then incubated at 37 °C for 90 minutes. The cells were plated on LB-agar (yeast extract, tryptone, NaCl and agar) plates containing 1μl/ml ampicillin and incubated overnight (~16 hours) at 37 °C. The pGEX4T-1 vector contains an ampicillin resistance gene which codes for β-lactamase, an

enzyme that inactivates ampicillin by cleaving the β-lactam ring in its structure, allowing for the selection of successful transformants (Chung *et al.*, 1989).

3.2.1. Plasmid purification and verification

A single colony from the transformants was selected from the LB-agar plates and cultured at 37 °C overnight in 2x YT media (1.0 g yeast extract, 1.6 g tryptone, 0.5 g NaCl per 100 ml dH_2O) containing 1µl/ml ampicillin. Plasmid DNA was purified from this culture using the GeneJet Kit DNA purification kit from Fermentas. Cells were lysed to release DNA and the plasmid DNA was subsequently purified from the chromosomal DNA and other cellular components using solutions from the kit. The purity and concentration of the DNA was assessed using Nanodrop TMRND-1000 spectrophotometer (Thermo Scientific, USA). The isolated DNA was sent to Inqaba Biotec (Pretoria, South Africa) for sequencing. The sequence was then aligned with the NCBI CLIC1 (NM_001288.4) sequence using the Blast2n alignment tool (http://blast.ncbi.nlm.nih.gov) at NCBI to confirm the presence of the CLIC sequence and the mutation required for truncating CLIC1 at amino acid 52.

3.2.2. GST fusion protein overexpression and purification

The overnight culture of the plasmid-bearing cells was re-cultured in 4 litres of 2YT/ampicillin media at 20°C until late log phase (OD_{600} ~ 0.7). Overexpression was induced with 1mM IPTG, the cells were allowed to grow at 20°C overnight (~16 hours) and harvested by centrifugation at 5000 rpm for 20 minutes. The cells were resuspended in STE buffer (10 mM Tris-HCl, 100 mM NaCl, 1 mM EDTA and 0.02% NaN_3), frozen overnight at -20°C and subsequently thawed at 4°C to allow for lysis. They were further lysed by sonication at a setting of 3, using 30 second bursts in half-second intervals (Sonicator from Misonix). Sonication is a method used to disrupt cells using high-frequency soundwaves (20-50 kHz) to agitate and lyse the cells (Belgrader *et al.*, 1999). To prevent heating of the sample (protein denaturing conditions) the sonication process was carried out on ice. The lysate was centrifuged at 15000 rpm for 30 minutes to pellet any unbroken cells and other cell debris leaving the proteins in solution (supernatant). The resulting supernatant was diluted twice with the equilibration buffer (10 mM Tris-HCl, 150 mM NaCl, 1 mM EDTA, 1 mM DTT, pH 8.0) for the GSH-Sepharose column and then loaded onto the GSH-Sepharose column that was pre-equilibrated with 10 column volumes of the equilibration buffer. GSH-sepharose is a GST-affinity matrix with GSH attached to the sepharose beads. The *Sj*GST tag of the

recombinant protein binds the GSH on the matrix (Smith and Johnson, 1988) whilst other proteins that cannot bind GSH pass through the column. The column was washed using ten column volumes of the equilibration buffer to remove any non-specifically bound proteins and the fusion protein was eluted using GST-elution buffer (50 mM Tris-HCl, 100 mM reduced GSH, pH 8.0) in fractions of 2 ml. The protein content of the fractions was quantified by absorbance spectrometry at 280 nm and the purity of the fractions assessed by SDS-PAGE using 16% polyacrylamide gels. SDS-PAGE is a method that separates proteins according to their size with the use of electrophoresis. SDS is added to the protein sample before it is loaded onto the gel. SDS is a detergent that denatures the structure of proteins by coating them to prevent refolding and conferring an overall negative charge to the protein molecule so that its movement through the matrix is based solely on size towards the positive electrode. The protein sample is then loaded into a polyacrylamide gel whose pores allow for the passage of the proteins. The proteins travel across the gel according to their size and the smallest proteins move faster and much further (Laemmli, 1970). The SDS-PAGE gels were stained with Coomassie blue. A pure protein forms one distinct band whose size can be evaluated using a molecular weight marker loaded into a separate well. Pure fractions of the fusion protein with an OD_{280} above 1.0 were pooled together.

3.2.3. Off-column thrombin digestion of fusion protein

Thrombin cleavage of GST fusion proteins is usually performed whilst the fusion protein is still bound to the GSH-affinity column resulting in the release of the target protein whilst the GST partner remains bound to the column. Attempts at on-column thrombin cleavage of the *Sj*GST-(β1-TMR) fusion protein were unsuccessful resulting in an incompletely digested fusion protein. Thus, the fusion protein was eluted from the GSH column and the fractions pooled together as described in Section 3.2.2. The protein stock was dialysed against thrombin cleavage buffer (10 mM Tris-HCl, 150 mM NaCl, 2.5 mM CaCl, 1 mM DTT, pH 8.4) in preparation for off-column thrombin digestion. Thrombin from human plasma was added to the fusion protein in thrombin cleavage buffer and incubated at 20°C for at least 16 hours with mild agitation. Thrombin is a site specific protease that cleaves proteins guided by a recognition sequence (Leu-Val-Pro-Arg-Gly-Ser) (Lottenberg *et al.*, 1981; Chang, 1985). The thrombin cleaves between the arginine and glycine residues, releasing the β1-TMR from the fusion protein with glycine and serine appended to the N-terminal of the β1-TMR. This cleavage results in a solution of β1-TMR, GST and thrombin. The success of the thrombim

digestion of the *Sj*GST-(β1-TMR) fusion protein was assessed using SDS-PAGE. The size of the β1-TMR protein is ~6 kDa (ProtParam, Gasteiger *et al.*, 2005) and because of its very small size, a modified version of SDS-PAGE was employed. Standard SDS-PAGE employs glycine buffers but a tricine system is preferred to resolve proteins smaller than 30 kDa and those with high hydrophobic content (Schägger and von Jagow, 1987). The two systems have different pKa values that define them as trailing ions relative to the electrophoretic mobility of the proteins. Sixteen percent polyacrylamide gels can resolve proteins ranging from 1-70 kDa, a mass range much narrower than that resolved by standard SDS-PAGE. In both methods, a pure protein should form one distinct band whose size can be evaluated using a molecular weight marker loaded into a separate well and the gels can be visualised using Coomassie blue or other modified staining methods. (Laemmli, 1970; Schägger, 2006). The thrombin-digestion mixture was analysed by SDS-PAGE using 16% acrylamide gels to confirm their purity and the size. Smaller proteins can easily diffuse out of polyacrylamide gels into the staining solution. Fixing of the proteins can be done to prevent this. The Tricine SDS-PAGE gels were first fixed using 10 mM ammonium acetate in 50% methanol and 10% acetic acid (Schägger& von Jagow 1987; Schägger, 2006) before staining with Coomassie blue.

In an effort to separate the β1-TMR peptide from the *Sj*GST, ultrafiltration was employed. This method uses membranes with pores of various size to separate proteins according to their size. The thrombin digestion mixture was filtered through a pm10 membrane with a molecular weight cut-off of 10 kDa to filter any proteins larger than 10 kDa i.e. *Sj*GST (26 kDa) and thrombin (37 kDa). The filtrate was then subsequently run through pm3 membrane with a molecular weight cut-off of 1 kDa to concentrate it. The protein content was assessed using absorbance spectrometry at 280 nm.

3.2.4. Size exclusion chromatography

To separate the β1-TMR from the thrombin cleavage mixture containing *Sj*GST and human plasma thrombin, size-exclusion chromatography was employed using the G-75 Sephadex size exclusion matrix. Size exclusion chromatography (SEC) by gel filtration separates molecules according to their size. The matrix is composed of beads with pores which can accommodate certain size molecules while molecules of a size greater than this remain in the mobile phase and are eluted first. The exclusion limit on the G-75 is 3 kDa- 80 kDa, meaning

molecules in this range enter the pores in the beads, the smallest molecules are able to enter more pores and are retained in the beads longer resulting in them eluting last. Blue dextran (2 000 kDa), chicken egg lysozyme (14 kDa), human albumin (40 kDa) and glutathione transferase A1-1 (52 kDa) were used as standards to determine the elution time of the contents of the thrombin cleavage mixture. Blue dextran is a polysaccharide of large molecular weight which is used to determine the void volume of the size-exclusion matrix: the volume at which the largest molecules will elute. The other standards were chosen because of their similar size to the components of the thrombin cleavage mixture: human plasma thrombin (37 kDa), *Sj*GST (52 kDa) and the β1-TMR (6 kDa).

3.3. Acquisition of synthetic TMR peptide

The TMR of CLIC1 is a 23 residue sequence in the N-domain (Cys24-Val46). The production of such a peptide using expression systems can prove difficult because of its size and hydrophobic properties. A 30 residue synthetic peptide encompassing Gly22 to Arg51 (Ac-GNSPFSQRLFMVLWLKGVTFNVTTVDTKRR-Am) and containing the TMR of CLIC1 was purchased from GL Biochem (Shanghai, China). The Cys24 residue was replaced by Ser24 to prevent oxidation and the formation of intermolecular disulfide bonds which would contribute to aggregation. The change to a serine would replace the hydrophobic thiol side chain of cysteine with a polar hydroxyl group. A mutation of Cys24 to Ala24 in CLIC1 has been shown to affect the redox activity and function of the channel but not membrane insertion and channel formation (Singh and Ashley, 2006). The peptide was designed with N- and C-terminal modifications, acetylation and amidation respectively, providing flanking peptide bonds that stabilise the peptide and create an environment similar to that the peptide would reside in, in the native protein.

3.4. Solubilisation of TMR peptide

To effectively solubilise the TMR peptide, the properties of the peptide needed to be known. The peptide sequence was analysed with ProtParam (Gasteiger *et al.*, 2005) as well as a peptide property calculator from innovagen (http://www.innovagen.se/custom-peptide-synthesis/peptide-property-calculator/peptide-property-calculator.asp). To solubilise the peptide, solvents generally recommended for solubilising synthetic peptides were utilised. The solvents included phosphate buffers, ethanol and methanol.

3.4.1. Peptide concentration determination

Absorbance spectroscopy can be used to assess both the purity and the concentration of the protein samples. Absorbance at 280 nm can be used to quantify proteins based on the amino acid residues that absorb light at this wavelength i.e. tyrosine and tryptophan. A series of dilutions of the TMR peptide solutions were prepared and their absorbances read at 280 nm from which a calibration curve of A_{280}(corrected) plotted against the dilution factor was constructed to aid in the determination of the peptide concentration.

The A_{280} readings were corrected for the buffer using the equation:

$$\mathbf{A_{280}(corrected) = (A_{280}(protein) - A_{280}(buffer))} \qquad \textbf{Equation 1}$$

The extinction coefficient (ε) is a measure of the extent a protein can absorb light at a specific wavelength. The molar extinction coefficient of the TMR peptide was determined from its amino acid sequence based on the molar extinction coefficient of the lone Trp35 in the TMR (Equation 2) (Perkins, 1986). The $\varepsilon 280$ for tryptophan has been shown to be solvent dependent, and is higher in alcohol solvents such as propanol but it does not vary significantly (Pace, 1995).

$$\mathbf{\varepsilon 280\ (M^{-1}cm^{-1}) = 5550\Sigma Trp + 1340\Sigma Tyr + 150\Sigma Cys} \qquad \textbf{Equation 2}$$
$$\mathbf{= 5550(1) + 1340(0) + 150(0)}$$
$$\mathbf{= 5550\ M^{-1}cm^{-1}}$$

The molar extinction coefficient together with the linear regression analysis of the calibration curve was used to determine the concentration of the TMR peptide using the Beer-Lambert law:

$$\mathbf{A = \varepsilon c l} \qquad \textbf{Equation 3}$$

where **A** is the absorbance, **ε** is the molar extinction coefficient of the peptide at wavelength 280 nm, **c** is the concentration of the peptide solution and ***l*** is the cuvette path length.

3.5. Characterisation of TMR peptide

To characterise the structure of the membrane-bound TMR, the structure of TMR peptide was studied in membrane-mimetic solvents using biochemical and biophysical methods.

3.5.1. Circular dichroism

Circular dichroism (CD) is a form of spectroscopy that measures the differences between the absorbance of left- and right circularly polarised light by proteins and can be used to characterise the secondary structure of proteins (reviewed by Woody, 1995). The absorption bands for the peptide backbone are found in the far-UV range (170 – 250 nm) while that of disulphide groups and aromatic amino acids are found in the near-UV range (250 – 300 nm). Equal amounts of the two types of polarised light are radiated into a solution containing the protein, and are absorbed in different amounts. The difference in absorbance is dependent on the wavelength and yields the CD spectrum for the sample. The secondary structural elements, alpha helices or beta sheets, have CD absorbance spectrums that are unique to them that can be used for reference when solving for unknown structures of protein sequences (Henessey *et al.*, 1981; Johnson, 1990; Provencher *et al.*, 1981). CD spectroscopy was used to assess the structure of the TMR peptide in membrane-mimetic solvents, predicted to be alpha-helical in the native protein when in the membrane. The model for membrane protein folding predicts that a TM peptide should retain its native structure when excised from its parent protein (Popot and Engelman, 1990).

All CD measurements were performed on a Jasco J-810 spectropolarimeter (Jasco, Japan). An average of 5 scans was recorded in the far-UV region (190 – 250 nm) at 200 nm/min with a data pitch of 0.1 nm, a response time of 1 second and a bandwidth of 2 nm to characterise the secondary structure of 10 μM TMR peptide at 20°C. All spectra were buffer-corrected and the raw signal in mdeg converted to mean residue ellipticity (MRE) [Θ] (deg.cm^2.dmol^{-1}) using the following equation:

$$[\Theta] = (100\,\theta)/cNl \qquad \textbf{Equation 4}$$

where θ is the raw signal in mdeg, **c** is the concentration of the protein (mM), **N** is the number of residues in the protein and ***l*** is the path length (Woody, 1995).

Native spectra were smoothed using the negative exponential function in Sigmaplot v. 11.0. Far-UV CD at 222 nm (**Θ222**) was also used to monitor changes in secondary structure during thermal unfolding experiments.

3.5.2. Fluorescence

3.5.2.1. Steady-state fluorescence

Fluorescence is the phenomenon by which a molecule emits radiation or light at a lower energy than the energy of the light absorbed. This is a result of the return of an unpaired electron from the excited to the ground state, transferring the excitation energy to the surrounding medium (Lakowicz, 1983). The side chains of two amino acids (tryptophan and tyrosine) exhibit significant intrinsic fluorescence. Both amino acids can be excited at 280 nm but tryptophan can be selectively excited at 295 nm. Tryptophan has the highest fluorescence quantum yield. The use of intrinsic fluorescence for the study of protein tertiary structure relies on the fact that the parameters of tryptophan emission depend on environmental factors such as solvent polarity and pH (Lakowicz, 1983; 1999). A highly exposed tryptophan in a folded structure has maximum fluorescence emission in the vicinity of 350 nm and an environment of reduced polarity results in a characteristic blue shift and tryptophan emits maximally at wavelengths shorter than 350 nm (Caputo and London, 2003; Lakowicz, 1999). The maximum fluorescence emission wavelength for a tryptophan residue is related to the extent of the exposure of the indole ring to the solvent and gives information about the tryptophan's packing and local environment (Lakowicz, 1999). The fluorescence of Trp35 in the TMR peptide was evaluated by exciting 10 μM TMR at 295 nm using a Perkin Elmer LS50-B spectrofluorometer. Measurements were performed in a quartz cuvette (1 cm pathlength) with a scan speed of 200 nm/min over wavelength range 295-450 nm using excitation and emission slit-widths of 3cm and a data pitch of 0.5 nm. All experiments were performed at 20°C and all data were buffer-corrected.

3.5.2.2. Acrylamide quenching

Acrylamide is a neutral, water-soluble and efficient quencher of tryptophan fluorescence. Acrylamide quenching is a technique that is used to gather information concerning the exposure and microenvironment of tryptophan residues in proteins. This is related to the tertiary packing of the protein in that environment (Eftink, 1991). Acrylamide quenching of the TMR peptide's intrinsic fluorescence was used to study the tertiary environment of Trp35

when it was in an environment representative of the membrane (2,2,2-Trifluoroethanol) and to give insight into the effect of pH (Phillips *et al.*, 1986). Acrylamide quenching is very sensitive to the degree of tryptophan accessibility to the solvent containing the acrylamide. Acrylamide is generally excluded from the hydrophobic interior of membranes or the hydrophobic interior of proteins. Any change in the tertiary structure of the TMR peptide around the tryptophan can be studied by observing by the degree which the tryptophan fluorescence is quenched by the acrylamide and whether this changes as the pH is changed. Quenching by Acrylamide was analysed using the modified Stern-Volmer equation:

$$F_0/F = 1 + K_{sv}[Q] \qquad \textbf{Equation 5}$$

where K_{sv} is the Stern-Volmer dynamic quenching constant and **[Q]** is the quencher (acrylamide) concentration (Eftink, 1991; Lakowicz, 1999).

3.5.3. Behaviour of TMR peptide in SDS micelles

Surfactants are amphiphilic molecules consisting of a long hydrocarbon tail and a hydrophilic headgroup which can change the properties of a polar solution, especially its ability to solubilise hydrophobic substances by the formation of micelles (Jelinek and Kolusheva, 2005). Sodium dodecyl sulphate is a surfactant that is used in membrane protein studies because of its ability to form micelles, small sphere-shaped structures with properties that resemble those of the membrane. SDS micelles form when a minimum bulk SDS concentration is reached (8 mM) which is the critical micelle concentration (CMC) of SDS (Garavito and Ferguson-Miller, 2001). SDS micelles provide an anionic, membrane-mimetic environment with a hydrophobic core and a polar surface. The anionic groups of SDS first bind to the cationic groups of amino acids like lysine while additional detergent molecules bind to hydrophobic domains through hydrophobic interactions resulting in an increase in helical structure of TM domains when in SDS solutions (Wu *et al.*, 1981; Wu and Yang, 1978). An electrostatic anchor such as SDS forms stable protein-detergent complexes that allow formation of a hydrophobic environment required for alpha-helix hydrogen bond network stabilisation. Varying concentrations of SDS (0-20 mM) in 5 mM phosphate buffer pH 5.5 were used to characterise the secondary structure of the TMR peptide in a micellar environment using far-UV CD. TMR peptide stock solution was added to SDS/phosphate buffer mixtures of SDS to a final concentration of 10 μM.

3.5.4. Effect of environment on the TMR peptide: pH and TFE studies

2,2,2-Trifluoroethanol (TFE) is a non-polar solvent with properties very similar to the membrane and is widely used as a membrane model system. TFE facilitates the formation of protein secondary structures that would not normally form in polar solutions but it cannot confer secondary structure (e.g. helices) on sequences that have no propensity to form such structures (Rohl *et al.*, 1996; Kumaran and Roy, 1999). TFE molecules coat the peptide, displacing water and removing alternate hydrogen-bonding partners to favour the formation and stabilisation of intra-peptide hydrogen bonds (Roccatano *et al.*, 2002). Different concentrations of TFE (0-100%) were used to create a non-polar environment for the TMR peptide to give insight into the structures formed by the peptide in the non-polar environment of the membrane interior.

TFE studies were performed at two pH conditions: pH 5.5 and pH 7.0, the pH representative of the membrane surface and the cytoplasm, respectively, representing the changing environment the peptide would encounter as it approaches the membrane. A TFE-independent study in aqueous solution at different pH values (5.0-8.5) as well as at different TMR peptide concentrations (5-35 μM) was carried out to investigate changes in the CD signal as a result of a change in structure and/or aggregation of the peptide. All solutions contained final concentrations of 5 mM phosphate buffer and 10 μM TMR peptide. Far-UV CD spectra (190-250 nm) were collected to observe the effect of these conditions on the secondary structure of the TMR peptide.

3.5.5. Stability studies

Protein stability refers to the thermodynamic stability of a protein or a peptide. This can be measured by the difference in Gibbs free energy, ΔG, between the folded (G_f) and the unfolded (G_u) forms of the protein or peptide. This is the activation energy required for the peptide to unfold and the larger and more positive ΔG, the more stable the peptide is to denaturation (Pace *et al.*, 1996, Baldwin, 2003). Peptide denaturation can be carried out by manipulating factors in the immediate environment of the peptide, such as pH and/or temperature or by using chemical denaturants.

Chemical denaturants unfold peptides either by forming hydrogen bonds with the peptide backbone and aromatic residues or by affecting the structure of the surrounding water

molecules thus altering the hydration of protein groups and weakening the hydrophobic effect (Bennion and Daggett, 2003). During the denaturation process, the hydrophobic core of the native state is initially solvated by water but the denaturant interacts preferably with non-native states to form the denatured state (Bennion and Daggett, 2003). Urea equilibrium unfolding of the TMR peptide was performed under the conditions mentioned in section 3.5.4., to determine the stability of the structure formed by the TMR peptide in the membrane. The stability of the TMR peptide was assessed by following its helical and fluorescent behaviour at increasing urea concentrations. 10 M urea was prepared in 5 mM phosphate buffer (pH 5.5 and pH 7.0) and used to make solutions containing urea concentrations from 0 M to 6 M in 40% TFE to which 10 μM TMR peptide was added. The change in ellipticity of the TMR peptide was observed at 222 nm using circular dichroism and the fluorescence of Trp35 was followed at 355 nm.

Thermal stability of the TMR peptide was also assessed using thermal unfolding. A solution containing 10 μM TMR in 40% TFE at either pH 5.5 or pH 7.0 was heated from 10-100°C while monitoring its ellipticity at 222 nm. The reversibility of the unfolding reaction was also assessed by cooling the sample after heating to allow refolding. The melting temperature of a protein whose unfolding is fully reversible is directly related to conformational stability and the thermodynamics of protein folding can be determined from it (Pace *et al.*, 2004).

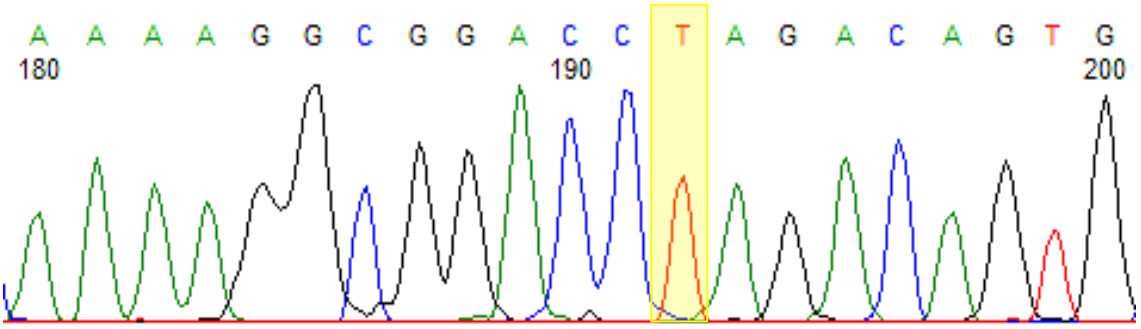
4. RESULTS

4.1. Purification of the β1-TMR peptide

4.1.1 DNA Sequencing

The pGEX-4T-1 plasmid containing the CLIC1 DNA was sent for sequencing at Inqaba Biotec (Pretoria, South Africa) to confirm the incorporation of the mutation that would yield CLIC1 truncated at Thr52, referred to as β1-TMR. The DNA sequence shows a T at nucleotide position 192 (Figure 7). This sequence shares 99% identity with the NCBI wild-type CLIC1 sequence (NM_001288.4) and changes the codon for Glu53 (GAG) into a stop codon (TAG) thus coding for the β1-TMR peptide.

A



B

```
Query       CCTTCAATGTTACCACCGTTGACACCAAAAGGCGGACCTAGACAGTGCAGAAGCTGTGCC
            ||||||||||||||||||||||||||||||||||||||||||||||||||||||||||||
CLIC1       CCTTCAATGTTACCACCGTTGACACCAAAAGGCGGACCGAGACAGTGCAGAAGCTGTGCC
```

Figure 7: Sequencing result of pGEX-CLIC1 plasmid
(**A**) Sequencing output of the mutated DNA shows a T at nucleotide position 192. (**B**) Blast alignment of sequenced DNA with CLIC1 from *homo sapiens* (NM_001288.4) shows that T has replaced a G in the wild-type CLIC1(yellow) and changes the codon for Glu53 (GAG) into a stop codon (TAG) (red box).

4.1.2. Protein expression and purification

The expression of the GST-(β1-TMR) fusion protein was carried out as described in 3.2.2. Purification of the GST-(β1-TMR) fusion protein was carried out using GSH affinity chromatography. Each step of the expression and purification was assessed using SDS-PAGE gels. Figure 8A shows an SDS-PAGE gel of the samples collected. After the overnight incubation with IPTG a protein of ~ 30 kDa is overexpressed (lane 2). This protein is soluble and present in the supernatant (lane 5). It binds to the GSH-Sepharose resin and is not present in the eluate (lane 6). A standard curve was constructed from the distance travelled by the molecular weight markers and was used to confirm the size of the fusion protein (Figure 8B). The molecular weight of the purified protein was determined to be ~31 kDa using the equation of the calibration curve ($y = 0.0105x + 2.2006$). This is in the expected size range for the GST (26 kDa) and β1-TMR (6 kDa) fusion protein. The protein content in the eluted fractions was evaluated using absorbance spectrometry (Figure 8C) and the purity of fractions with an A_{280} value greater than 1 was assessed using SDS –PAGE (Figure 8D).

Off-column thrombin digestion was performed to separate β1-TMR from the GST as earlier experiments had shown that the fusion protein could not be cleaved while bound to the GSH-Sepharose resin. Thrombin digestion of the fusion protein was assessed using Tris-Tricine SDS-PAGE. This resulted in 2 proteins of molecular weights ~26 kDa and ~6 kD, indicating that the β1-TMR peptide had been successfully cleaved from the GST (Figure 9).

Various methods, including size exclusion chromatography, hydrophobic interaction chromatography, ultrafiltration and reloading the digestion mix onto the GSH-affinity column were used in an attempt to separate the β1-TMR peptide from the GST. However, these methods proved unsuccessful as the β1-TMR peptide could not be visualised using polyacrylamide gels or absorbance readings. Therefore, no characterisation work was done on the β1-TMR peptide.

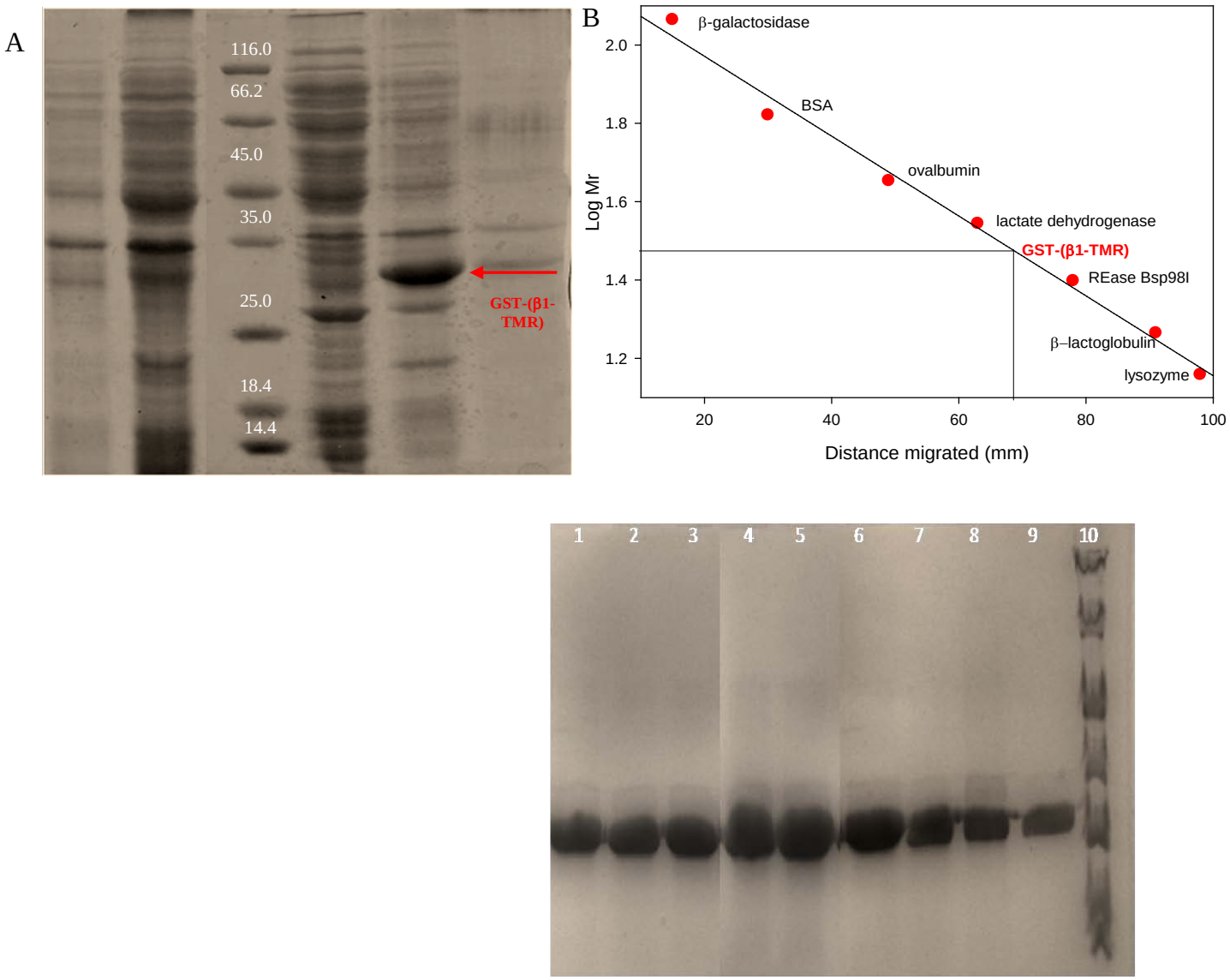


Figure 8: Expression and purification of the GST-(β1-TMR) fusion protein

(**A**) SDS-PAGE gel to evaluate the purity of the protein at each stage of the purification process, Lanes 1: pre-induction; 2: post-induction; 3: molecular weight marker; 4: pellet; 5: supernatant; 6: loading flow-through (**B**) Standard curve for the determination of molecular weight of the fusion protein using the molecular weight standards: β-galactosidase (116kDa); bovine serum albumin (66.2 kDa); ovalbumin (45 kDa); lactate dehydrogenase (35 kDa); REase Bsp98I (25 kDa) β-lactoglobulin (18.4 kDa) and lysozyme (14.4 kDa) . The position of the fusion protein on the standard curve is shown in black and the molecular weight of the fusion protein was calculated to be 31 kDa. (**C**) Elution profile of fusion protein off the GSH-Sepharose column (**D**) SDS- PAGE gel Lanes 1-9: Fractions 10-18 from elution profile (C); Lane 10: Molecular weight marker.

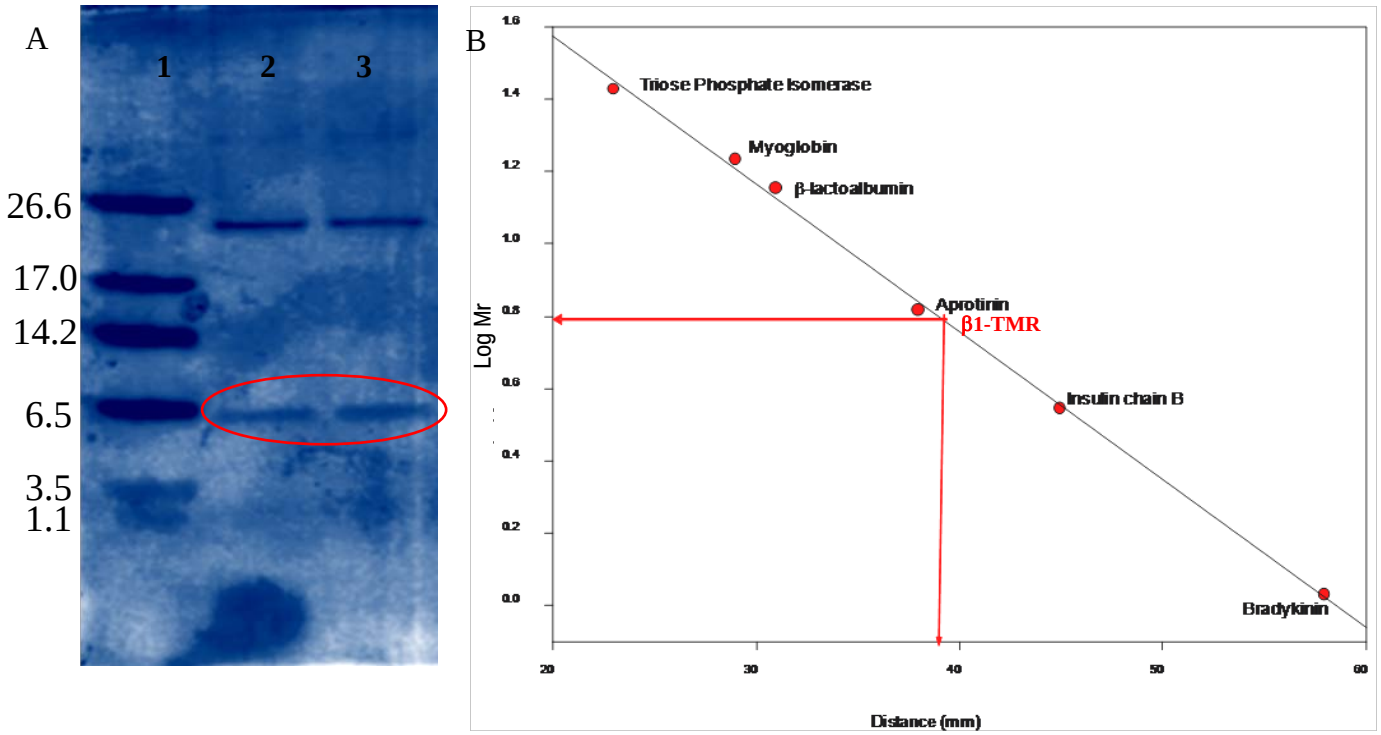


Figure 9: Thrombin cleavage of the GST-(β1-TMR) fusion protein
(**A**) 16% Tricine SDS PAGE. Lanes 1: molecular weight marker, 2: thrombin digestion mix, 3: thrombin digestion mix. (**B**) Standard curve constructed from the mobilities of molecular mass standards triose phosphate isomerise (26.6 kDa); myoglobin (17 kDa); β-lactoglobulin (14.2 kDa); aprotinin (6.5 kDa); insulin chain B (3.5 kDa) and bradykinin (1.1 kDa) on 16% Tricine SDS PAGE, indicating the position of β1-TMR in red as 6 kDa.

4.2. Solubilisation of the TMR peptide

The TMR peptide was obtained from GL Biochem (Shanghai, China) as a lyophilised powder. Mass spectrometry analysis from the synthesis report indicated that the TMR was >95% pure. The lyophilised TMR peptide needed to be solubilised for the characterisation experiments. The optimal solvent would effectively dissolve the peptide at high concentrations which allowed the use of small volumes of aliquots in order to minimise the effect of the initial solvent. The solvent would also be compatible with the techniques to be used in this study. A number of aqueous and organic solvents were tested to find a suitable solvent by adding the peptide to the solvents to a final concentration of 100 µM. The peptide solutions were centrifuged to pellet peptide that was not soluble and the concentration of the TMR peptide in the supernatant was determined by UV absorption and used as a measure of its solubility in the solvent. CD spectra were also recorded in the far-UV region to assess the secondary

structure of the TMR peptide in the various solutions as well as the suitability of the solvent for circular dichroism spectroscopy.

Analysis of the TMR peptide sequence using ProtParam, an online tool that computes the physical and chemical parameters of proteins (Gasteiger *et al.*, 2005), revealed a GRAVY (grand average of hydropathy) score of -0.2. The GRAVY index can be used as a measure of protein solubility, and a negative GRAVY score usually indicates a hydrophilic peptide that is soluble in polar solvents (Kyte and Doolittle, 1982). The analysis also indicated that the peptide had a pI of 12.24 and was a basic peptide with a charge of +4 between pH 5 and 9. Peptide manufacturers recommend that basic peptides, first be solubilised in aqueous solution. Electrostatic forces are crucial in keeping TM peptides soluble and factors such as ionic strength and pH of the buffer solution have to be carefully chosen. An increase in ionic strength resulting in the weakening of repulsive electrostatic forces has been shown to increase the risk of TM peptide aggregation (Lazarova et al., 2004). Low concentration sodium phosphate buffer was chosen as the polar solvent to be used in our study, as high concentration buffer was observed to interfere with the signal from far-UV CD measurements in earlier experiments.

The far-UV CD spectrum of the TMR peptide in 5 mM sodium phosphate buffer (pH 7.0) before centrifugation shows a secondary structure characterised by a minimum at ~215 nm (Figure 10), a pattern similar to that observed for beta-sheet aggregates (Arutyunyan *et. al.*, 2001; Compton *et.al*., 1987). The TMR peptide concentration of the supernatant from the solubilised in 5mM phosphate buffer was very much near zero (not shown) and the supernatant after centrifugation does not show any secondary structure (Figure 10) suggesting that no peptide remained in solution. The TMR peptide contains a large number of hydrophobic residues (40%) which can associate by hydrophobic interaction in an aqueous environment (Kauzmann, 1959) reducing their contact with and excluding the solvent (Tanaka, 2001) which will decrease its solubility in polar solvents and cause it to aggregate. This is not unusual as TM peptides often form extremely stable beta-sheet aggregates in aqueous solutions. These aggregates may even resist harsh detergents like SDS and therefore are of limited use for further investigations. TM peptides derived from receptor tyrosine kinases (Neu and ErbB2), exhibited CD spectra typical of beta-structured aggregates that persisted even in SDS–polyacrylamide gel electrophoresis (SDS-PAGE). Only after dissolving the lyophilised peptides in a chloroform/formic acid/acetic acid/TFE (2:1:1:1)

mixture could the TM peptides be characterised in membrane-mimetic systems (Bordag and Keller, 2010; Jones et al., 2000).

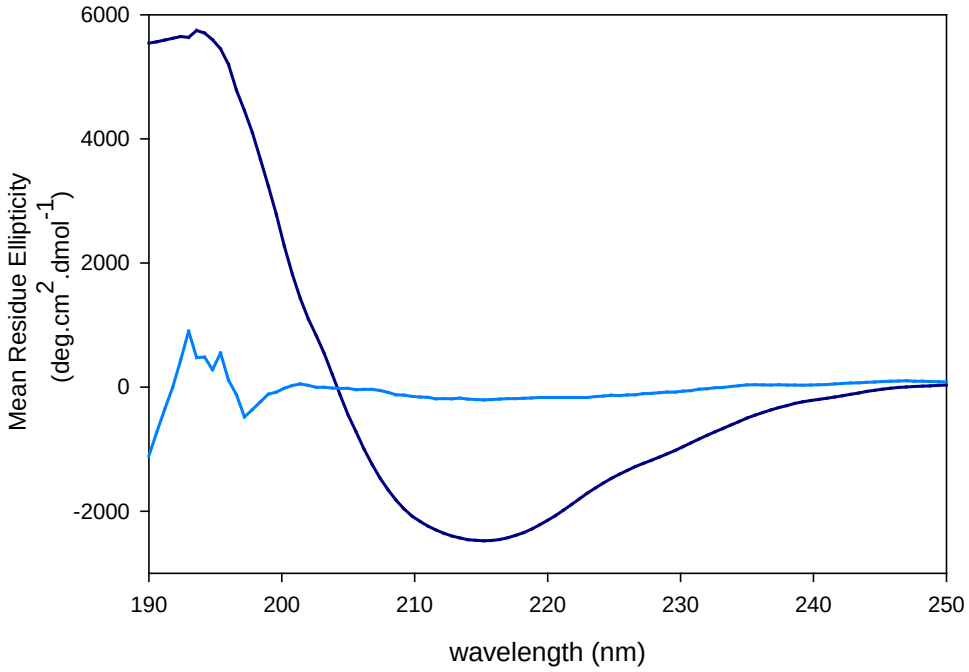


Figure 10: Far-UV CD spectra of the TMR peptide in aqueous buffer.
The TMR peptide in 5 mM sodium phosphate buffer, pH 7.0 at 20 °C before (dark blue) and after (light blue) centrifugation. The TMR peptide is not soluble in aqueous buffer. Data were plotted with Sigmaplot v. 11.0 and the spectra smoothed using the negative exponential method.

Organic solvents, due to simplicity of their chemical make up, have been applied in peptide research for over half a century with great success despite their poor resemblance to the membrane (Goodman and Rosen, 1964). In addition to being good solvents for hydrophobic peptides, most organic solvents induce and/or stabilise secondary structures that are intrinsic to the peptide (Buck, 1998; Katragadda *et al.*, 2001a,b; Roccatano *et al.*, 2002). Ethanol and methanol were tested for solubilising the TMR peptide, these organic solvents are generally recommended for peptide solubilisation (McMullen *et al.*, 1971).

Solubility of the TMR peptide in 100% ethanol was limited and the peptide formed aggregates that were recovered by centrifugation. The resulting solution had a low peptide concentration (~ 3 μM) as determined by UV absorbance (Figure 10A) and the far-UV CD spectrum shows alpha-helical secondary structure with minima at 222 nm and 208 nm and a

maximum ~190 nm (Figure 11B). Although the TMR peptide was soluble in ethanol to some extent, ethanol was not suitable for making a high concentration TMR peptide stock solution.

Solubilisation of the TMR peptide in methanol was successful, with no aggregates recovered after centrifugation. The peptide concentration of the supernatant calculated from the linear fit of the A280 measurements from the dilutions of the TMR peptide solution was close to that weighed out (~ 100 μM). High concentrations of methanol are routinely used to solubilise membrane peptides (Zhang *et al.,* 2007) and the far-UV circular dichroism spectrum of the TMR peptide in 100% methanol indicates alpha-helical secondary structure, with minima at 222 nm and 208 nm and a maximum at ~190 nm (Johnson, 1990) (Figure 12B). Due to its ability to completely solubilise the TMR peptide and its compatibility with far-UV circular dichroism, methanol was chosen to be the primary solvent.

2,2,2-Trifluoroethanol (TFE) is routinely used to promote the formation of secondary structure in peptides and as a membrane mimetic for the study of transmembrane peptides (Roccatano *et al.,* 2002; Tamburro *et al.,* 1968). TFE is also used as a solvent in nuclear magnetic resonance (NMR) to solve the solution structures of peptides (Clore *et al.,* 1986; Marion *et al.,* 1988). These studies often utilise TFE in conjunction with an aqueous solvent. TFE was selected as a membrane mimetic for the study of the TMR peptide. TFE binary mixtures form clathrate hydrate structures, where single TFE molecules are surrounded by a large number of water molecules (Buck, 1998). The immobilisation of water in these structures limits the amount of water molecules available in solution to interact with the peptide backbone leading to high local concentrations of TFE molecules around the peptide (Klaus *et al.,* 1998; Popa *et al.,* 2004; Roccatano *et al.,* 2002). It was decided that the TFE/buffer mixture would be used for this study as this also allowed for the regulation of pH which would be implemented in the subsequent experiments.

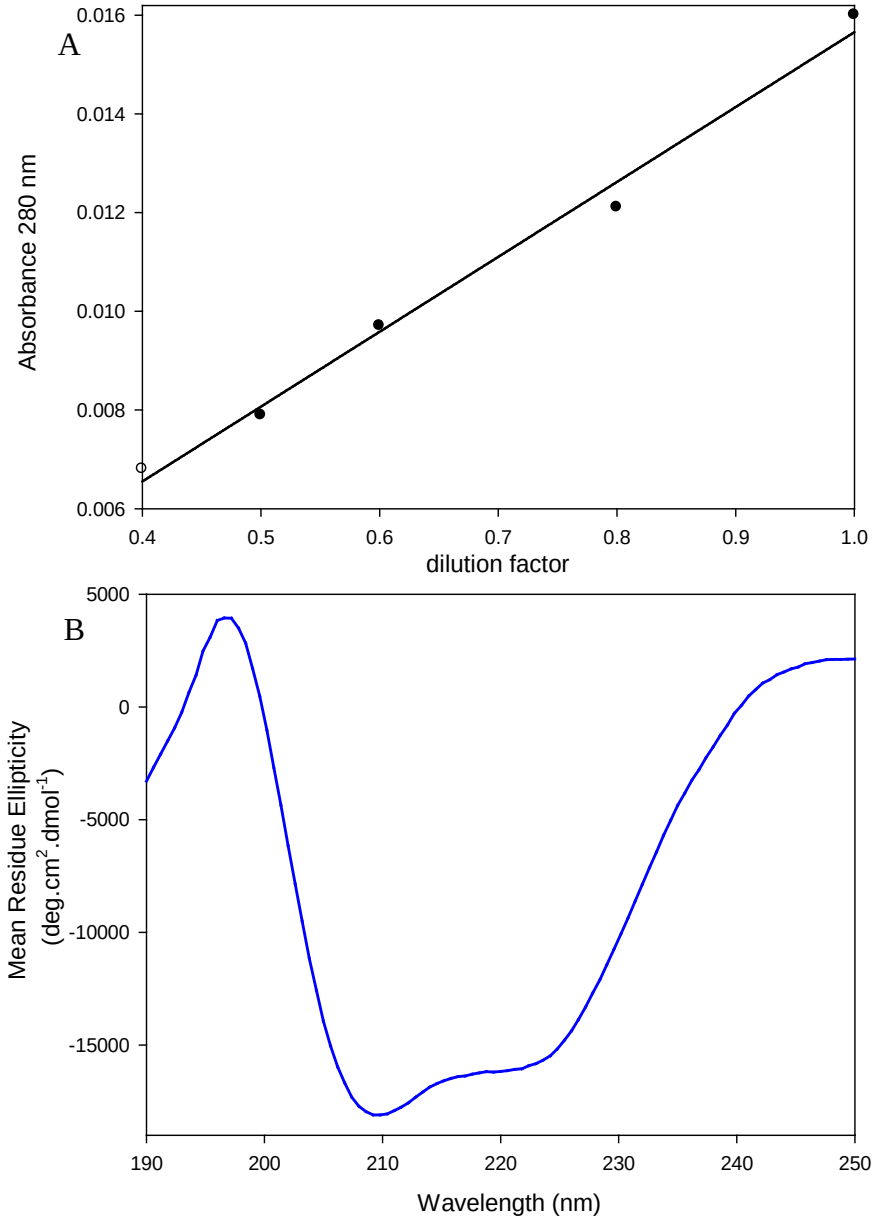


Figure 11: The TMR peptide in ethanol

(**A**) The absorbance of serial dilutions of the TMR peptide in 100% ethanol measured at 280 nm. The concentration was calculated as ~ (R^2 = 0.997). The TMR peptide has limited solubility in absolute ethanol. (**B**) Far-UV CD spectrum of 3 μM TMR peptide in 100% ethanol, at 20 °C after centrifugation shows alpha-helical secondary structure. Data were plotted with Sigmaplot v. 11.0 and the spectra smoothed using the negative exponential method.

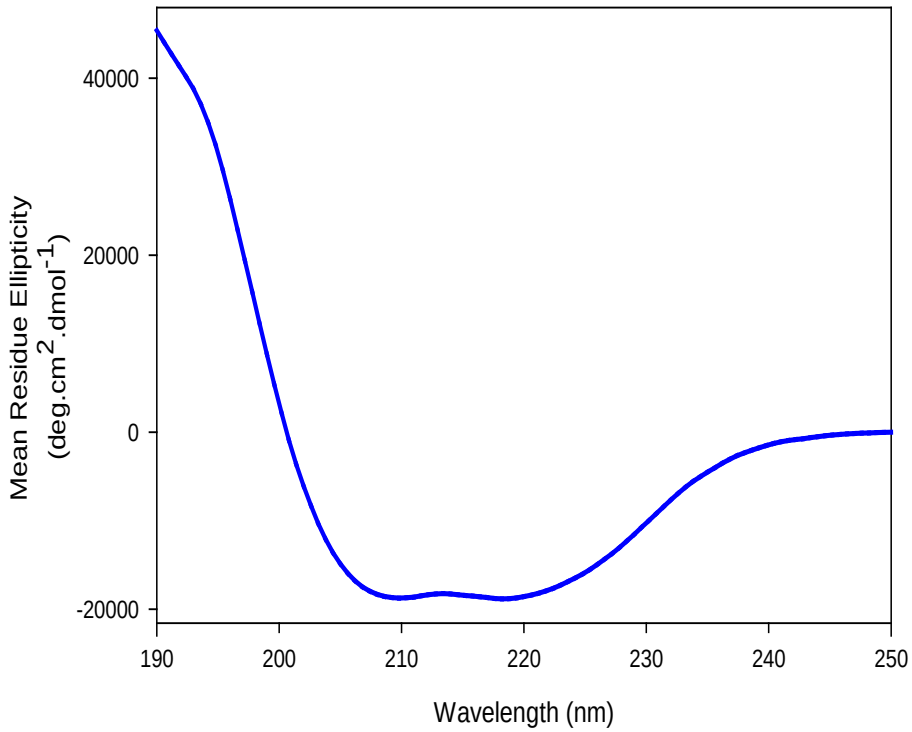


Figure 12: Far-UV CD spectra of the TMR peptide in methanol.
The TMR peptide in 100% methanol at 20°C. Secondary structure of the TMR peptide is alpha-helical in methanol. Data were plotted with Sigmaplot v. 11.0 and the spectra smoothed using the negative exponential method.

Methanol has been shown to reduce the structural content of peptides in TFE mixtures (Ganesh and Jayakumar, 2002; Planque *et al.*, 2007). Since methanol was chosen as the primary solvent for the TMR peptide, the effect of methanol concentration on the secondary structure of the TMR peptide in TFE/buffer mixtures was studied to determine a methanol concentration which would not interfere with the effect of TFE. The results indicate that increasing methanol concentration reduces the secondary structure observed in the TFE/buffer mixtures with the highest secondary structure observed at 2% methanol (Figure 13B). A high concentration stock solution of the TMR peptide was prepared in 100% methanol so that all samples used in this study contained a final concentration of 2% methanol.

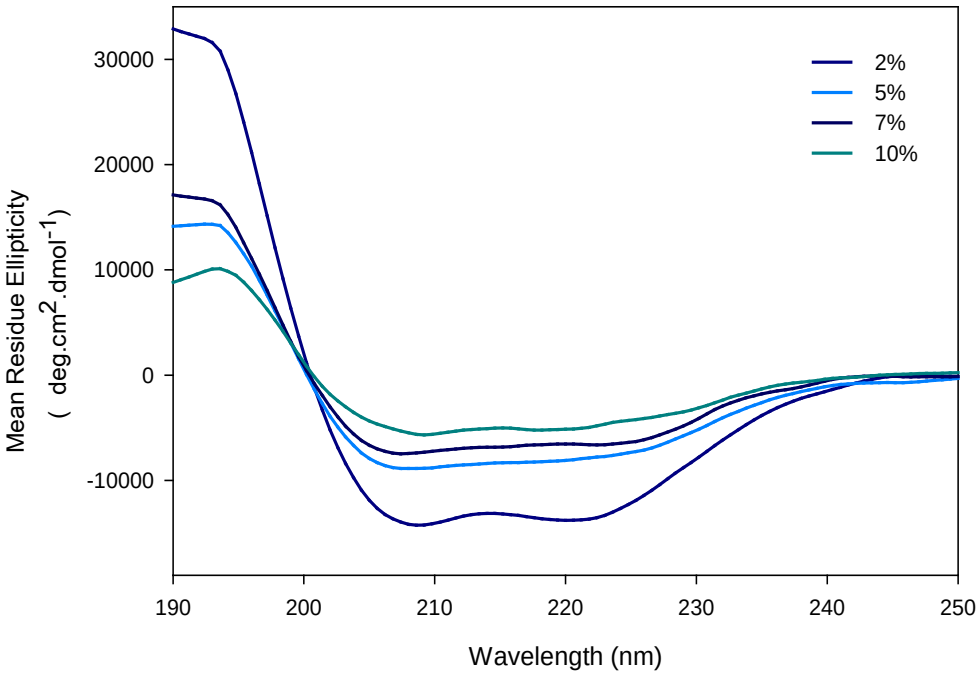


Figure 13: Far-UV CD spectra of the TMR peptide in 50% TFE
The TMR peptide in 50% (v/v) TFE/buffer (5 mM sodium phosphate buffer, pH 7) mixtures with varying concentrations of methanol at 20°C. Data were plotted with Sigmaplot v. 11.0 and the spectra smoothed using the negative exponential method.

4.3. Characterisation of the TMR peptide

To characterise the structure of the TMR peptide in a non-polar environment as is the case in the membrane, the secondary structure of the TMR peptide was studied using circular dichroism, as a function varying TFE concentrations in TFE/buffer mixtures. The mean residue ellipticity (MRE) at 222 nm, used as a measure of helical structure, was plotted against TFE concentration (Figure 14B). A decrease to a more negative value of MRE indicates an increase in secondary structure. At low concentrations of TFE (0-10%) the TMR peptide has very little secondary structure. Increasing the concentration of TFE from 10% to 40% transforms the TMR peptide from unstructured to an alpha-helical form. Further increase of TFE concentration beyond 40% TFE has no significant effect on the helical content of the TMR peptide. The effect of TFE is said to be saturated at low concentrations of TFE (~30%), where the TFE molecules are localised around ~80% of the peptide backbone (Imai *et al.*, 2009; Roccatano *et al.*, 2002). Thus all subsequent experiments were performed in 40% TFE. In the TFE study, there is a transition from a conformation that is almost devoid of any secondary structural elements to one that is characterised by high alpha-helical content

upon the addition of TFE. This resembles a two-state transition that is also evidenced by the presence of an isodichroic point at ~200 nm (Figure 14A).

To determine the content of the secondary structure formed by the TMR peptide in TFE/buffer mixtures, the circular dichroism spectrum at 40% TFE was analysed using Dichroweb (http://dichroweb.cryst.bbk.ac.uk/html/home.shtml), an online server for the deconvolution of circular dichroism data (Whitmore and Wallace, 2004). The server allows for the input of raw CD spectral data that can be analysed using a number of algorithms. The algorithm uses reference data sets of CD data of proteins with known structure and gives an output of a structural content that best fits the input data (Figure 15). The results indicate that in 40% TFE, the TMR peptide has a helical content of ~52% with ~ 26 % of the peptide unordered and 7% and 15% in strand and turn conformation, respectively (Table 1).

The self association of peptides, whether by aggregation or oligomerisation has been shown to increase with increasing peptide concentration (Juban *et.al.,* 1997). This self-association can be monitored by far-UV CD and would result in an increase in the helical structure i.e. far-UV signal. To ensure that the far-UV signal observed for the TMR peptide was not a result of aggregation, the effects of peptide concentration on the TMR peptide structure formed in 40% TFE/ buffer mixtures was investigated by monitoring the secondary structural content of the TMR peptide at different peptide concentrations. The resulting far-UV CD spectra show no significant change in the alpha-helical secondary structure of the TMR peptide as the concentration is increased (Figure 16).

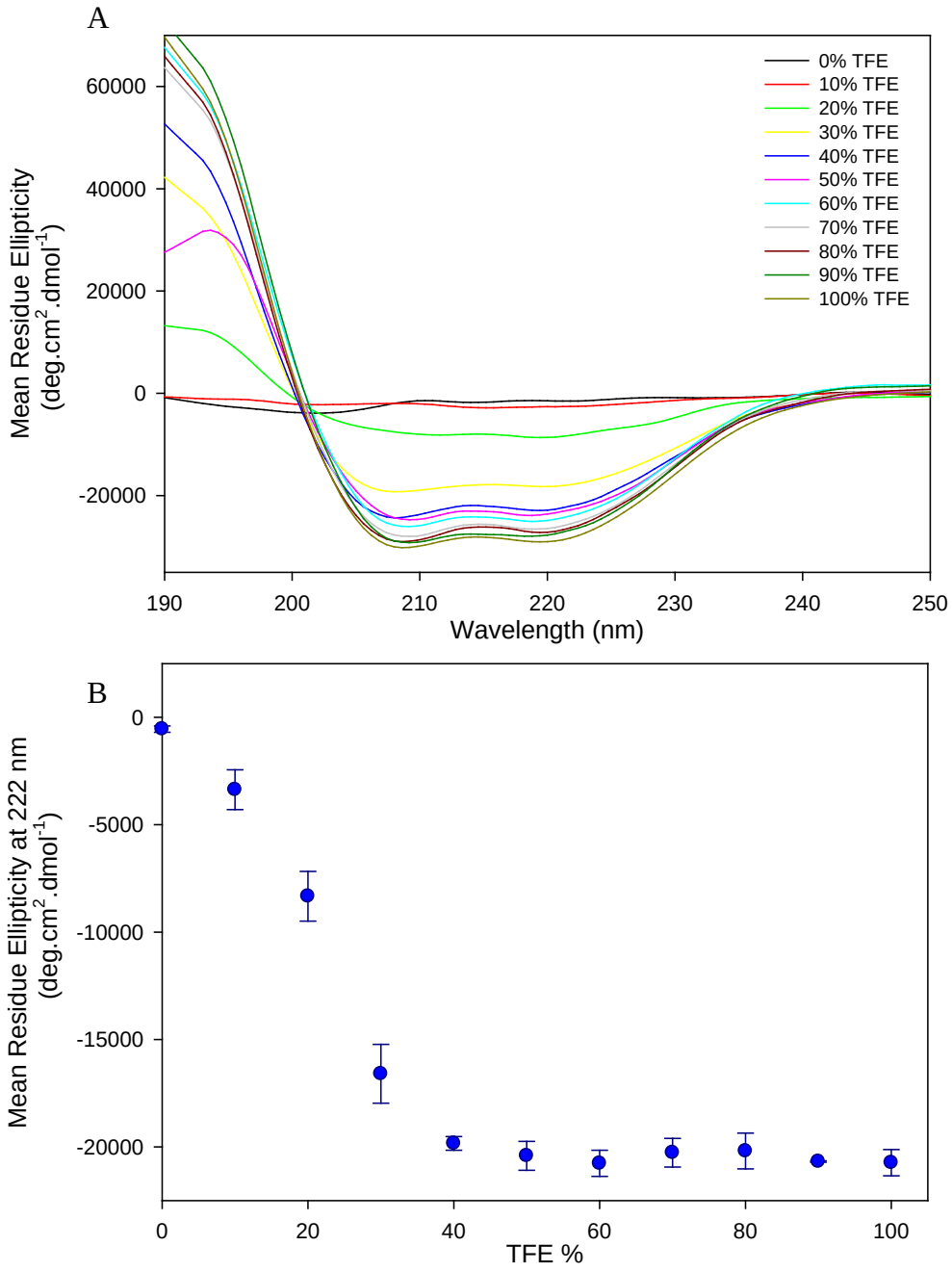


Figure 14: Far-UV CD spectra of the TMR peptide as a function TFE concentration
(**A**) Circular dichroism spectra of the TMR peptide in various TFE/buffer (5mM sodium phosphate buffer, pH 7) mixtures (% v/v) at 20°C. (**B**) The MRE at 222 nm of the TMR peptide as a function of TFE concentration indicates a two-state process from an unfolded to a helical form. Data were plotted with Sigmaplot v. 11.0 and the spectra smoothed using the negative exponential method.

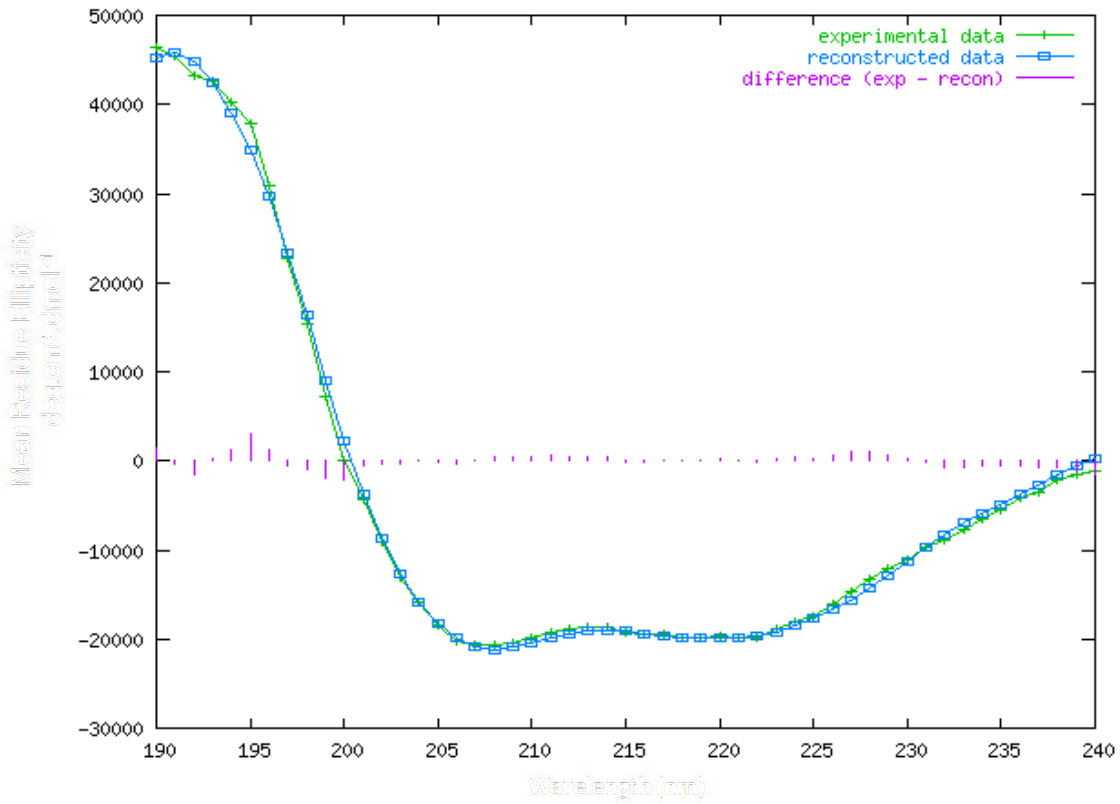


Figure 15: Dichroweb analysis of the TMR peptide in 40% TFE
Dichroweb output for the deconvolution of the CD spectrum of the TMR peptide in 40% (v/v) TFE/5 mM sodium phosphate buffer, pH 7. The fit has an NRMSD of 0.031.

Result	Helix1	Helix2	Strand1	Strand2	Turns	Unordered	Total
1	0.342	0.174	0.029	0.038	0.154	0.263	1
2	0.373	0.170	0.036	0.033	0.128	0.259	0.999

Table 1: Secondary structure composition of the TMR peptide in 40% TFE
Estimated structural content of the TMR peptide, Result 1: Closest matching solution with all proteins; Result 2: Average of all matching solutions. The TMR peptide is estimated to contain ~53% helicity at 40% TFE. Generated using Dichroweb (Whitmore and Wallace, 2004) with the CONTIN algorithm (VanStokkum *et al.*, 1990) and reference data set 4.

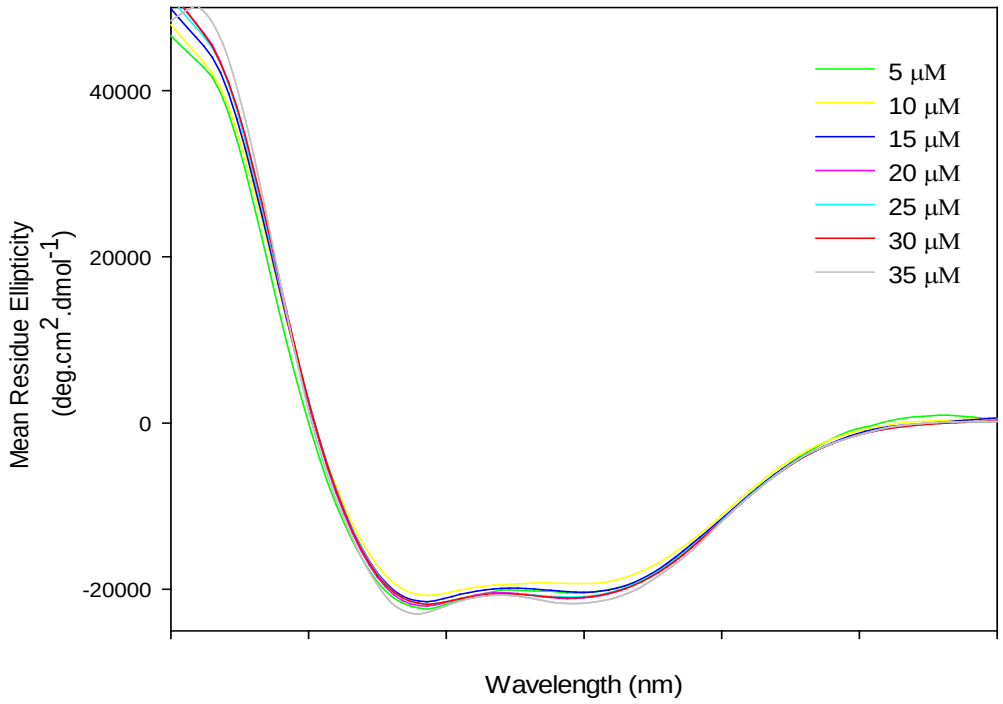


Figure 16: Effect of concentration on the secondary structure of the TMR peptide
Circular dichroism spectra of the TMR peptide in 40% (v/v) TFE/buffer (5 mM sodium phosphate buffer, pH 7) mixtures at varying TMR peptide concentrations (5 μM - 35 μM) at 20°C. Data were plotted with Sigmaplot v. 11.0 and the spectra smoothed using the negative exponential method.

Sodium dodecyl sulphate (SDS) is an anionic detergent often used as a membrane mimetic to study the membrane structure of transmembrane helices (Tulumello and Deber, 2009). SDS is able to form micelles at concentrations of 8 mM or more (Mukerjee and Mysels, 1971) in which transmembrane peptides adopt a secondary structure similar to that in the lipid bilayer (le Maire *et al.*, 2000; Lauterwein *et al.*, 1979). SDS was used as a membrane mimetic to characterise the structure of the TMR peptide. The mean residue ellipticity (MRE) at 222 nm, used as a measure of helical structure, was plotted against SDS concentration (Figure 17B). An increase in the negative ellipticity value indicates an increase in secondary structure. The helical content of the TMR peptide in SDS increases as the concentration of SDS is increased but no further increase is observed at SDS concentrations above 12 mM SDS (Figure 17A and B). Analysis of the structure content of the TMR peptide at 12 mM SDS using Dichroweb (Figure 18) indicates that the TMR peptide is only ~24 % helical with ~ 29 % of the peptide unordered and 27% and 20% in strand and turn conformation, respectively (Table 2).

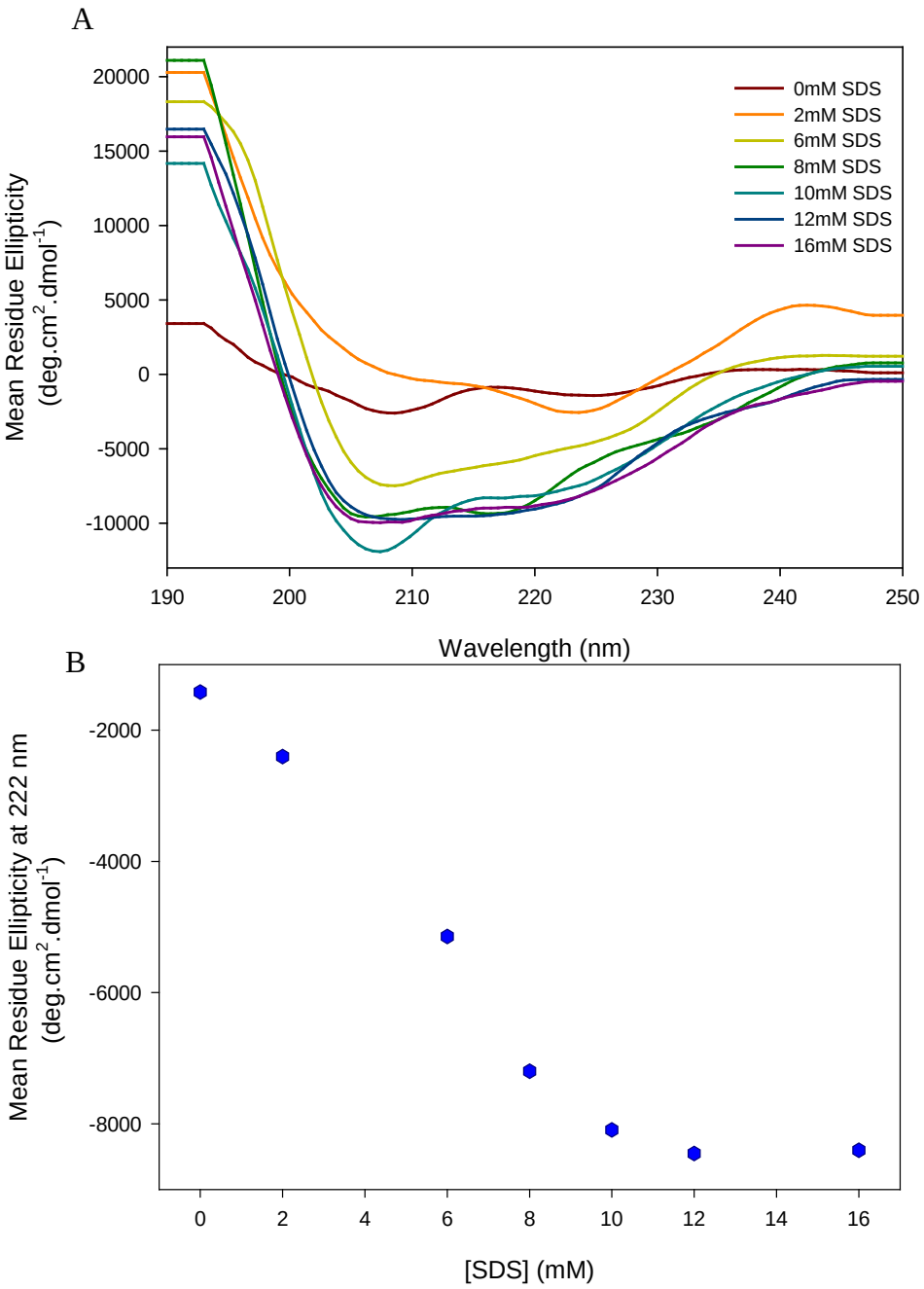


Figure 17: Far-UV CD of the TMR in SDS

(**A**) The TMR peptide in varying concentrations (0-16 mM) of SDS (5mM sodium phosphate buffer, pH 7) at 20°C and (**B**) The MRE at 222 nm of the TMR peptide as a function of SDS concentration. Data were plotted with Sigmaplot v. 11.0 and the spectra smoothed using the negative exponential method.

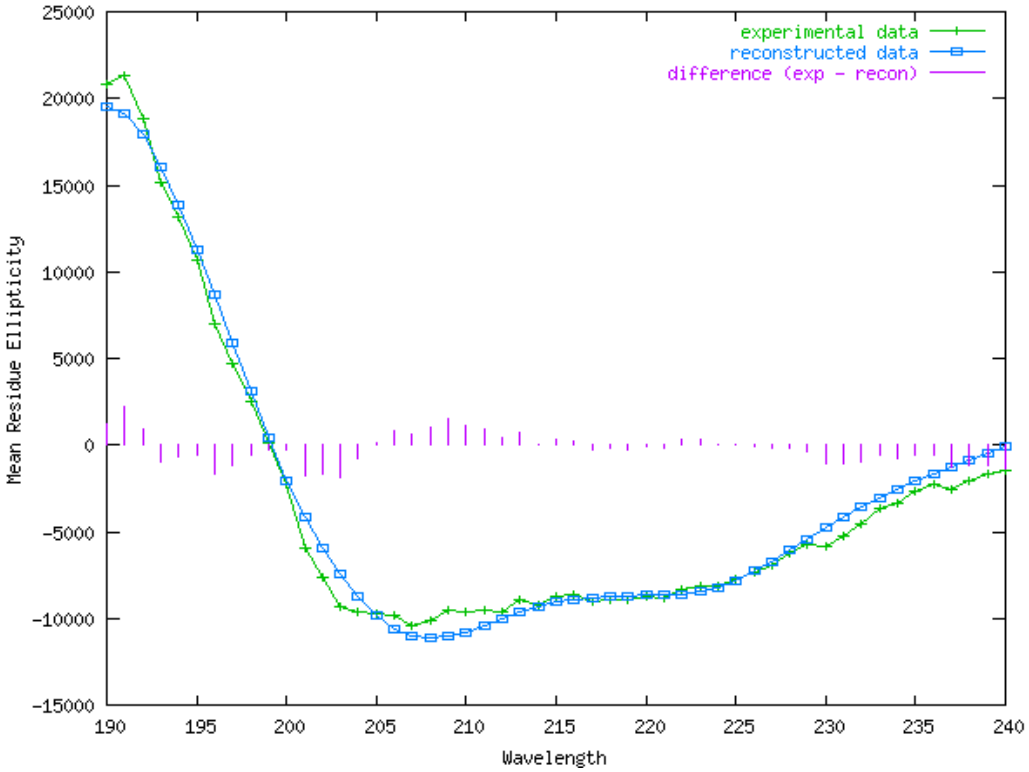


Figure 18: Dichroweb analysis of theTMR peptide in 16 mM SDS
Dichroweb output for the deconvolution of the CD spectrum of the TMR peptide in 16mM SDS/5 mM sodium phosphate buffer, pH 7. The fit has an NRMSD of 0.101.

Result	Helix1	Helix2	Strand1	Strand2	Turns	Unordered	Total
1	0.145	0.096	0.173	0.100	0.198	0.288	1
2	0.119	0.103	0.116	0.097	0.236	0.329	1

Table 2: Secondary structure compositionof theTMR peptide in 16 mM SDS
Estimated structural content of the TMR peptide, Result 1: Closest matching solution with all proteins; Result 2: Average of all matching solutions. The TMR peptide is estimated to contain ~24% helicity at 16 mM SDS. Generated using Dichroweb (Whitmore and Wallace, 2004) with the CONTIN algorithm (VanStokkum *et al.,* 1990) and reference data set 4.

4.3.1. pH- dependence

For CLIC1 to be able to insert into the membrane, it has to move from the cytoplasm to the membrane surface. Therefore, the pH that CLIC1 encounters changes from ~7.4 to ~5.5 (Menestrina *et al.*, 1989; van der Goot *et al.*, 1991). This change in pH environment is thought to be one of the contributing factors for the structural transition of CLIC1 into a membrane form (Fanucchi *et al.*, 2008; Stoychev *et al.*, 2009). The effect of pH on the secondary structure of the TMR peptide was studied in 40% TFE. The helical structure of the

TMR in TFE is not affected by a change in pH. The only change is a small reduction in helical content observed at pH 5.0 (Figure 19).

The transmembrane region of CLIC1 contains a tryptophan residue at position 35. To determine if pH would affect the tertiary structure of the TMR peptide, the fluorescence of the peptide was studied in 40% TFE at pH 5.5 and 7.0. Acrylamide quenching experiments were performed and compared to that of *N*-acetyl tryptophanamide (NATA). At pH 5.5, the K_{SV} values obtained were 13.3 M^{-1}(±0.2) for NATA and 12.1 M^{-1}(±0.1) for the TMR peptide (Figure 20A) and at pH 7.0, the K_{SV} values obtained were 12.9 M^{-1} (±0.1) for NATA and 9.8 M^{-1}(±0.1) for the TMR peptide (Figure 20B). There appears to be no significant difference in the environment of Trp35 in the TMR peptide between pH 5.5 and pH 7.0.

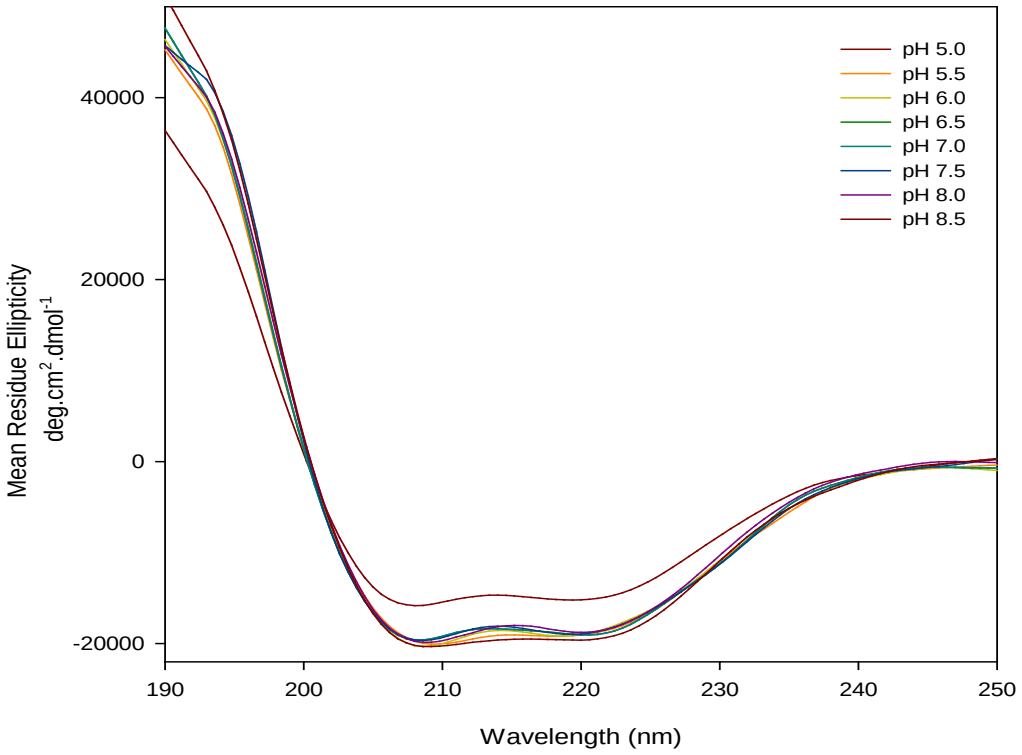


Figure 19: Effect of pH on the secondary structure of the TMR peptide in 40% TFE
Circular dichroism spectra of the TMR peptide in 40% (v/v) TFE/buffer (5 mM sodium phosphate buffer, pH 5.5) mixtures at different pH (5.0-8.5) at 20°C. Data were plotted with Sigmaplot v. 11.0 and the spectra smoothed using the negative exponential method.

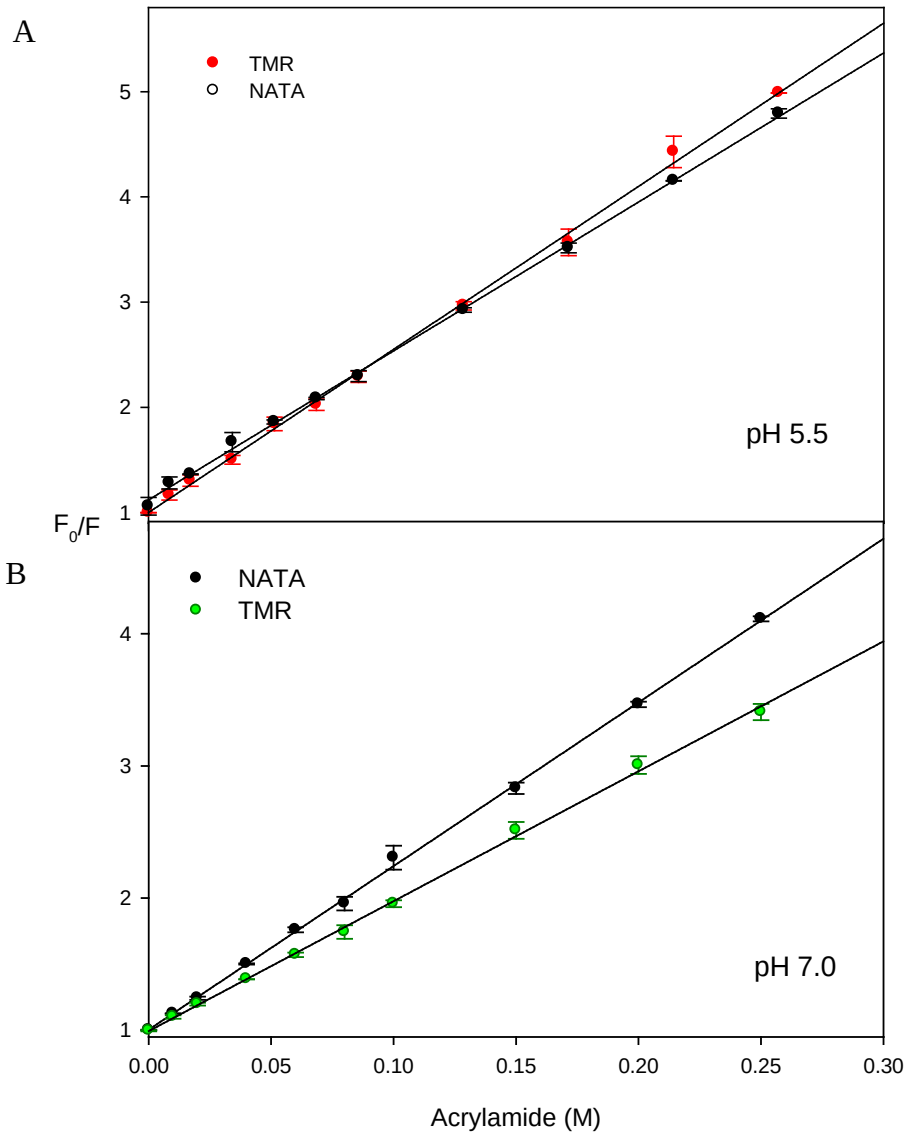


Figure 20: Acrylamide quenching of the TMR peptide
(**A**) pH 5.5, the K_{SV} values obtained were 13.3 M^{-1}(±0.2) for NATA (black) and 12.1 M^{-1}(±0.1) for TMR peptide (red) and (**B**) pH 7.0, 12.9 M^{-1} (±0.1) for NATA (black) and 9.8 M^{-1}(±0.1) for the TMR peptide (green) in 40% TFE/buffer (5mM sodium phosphate) at 20°C. Data were plotted with Sigmaplot v. 11.0 and fitted with linear regression.

4.3.2. Stability

The stability of the TMR peptide in a membrane environment was studied using chemical and thermal denaturation. Thermal unfolding of the peptide in 40% TFE showed that the helical content of the TMR peptide was gradually decreased as the temperature was increased (Figure 21A). The unfolding of the TMR peptide occurs over a large temperature range with

~20% of the structural content observed at 20°C remaining at 100°C. This denaturation is reversible and the TMR peptide recovers its initial structure upon cooling (Figure 21A insert). Chemical denaturation of the TMR peptide with urea also showed a gradual, almost linear unfolding curve. The helical structure of the TMR peptide starts to unfold as soon as urea is added and continues to unfold, until ~ 50% of the initial helical structure remains at 6 M urea (Figure 21B). Experiments of up to 8 M urea could not be performed because the requirement for 40% TFE in the reaction mixture limited the amount of 10 M urea stock that could be added to the reaction mixture.

The unfolding data could not be fit to an unfolding model as computational methods require defined baselines of the native and denatured states from which the unfolding can be compared to determine the thermodynamic parameters of the unfolding process (Breslauer, 1995).

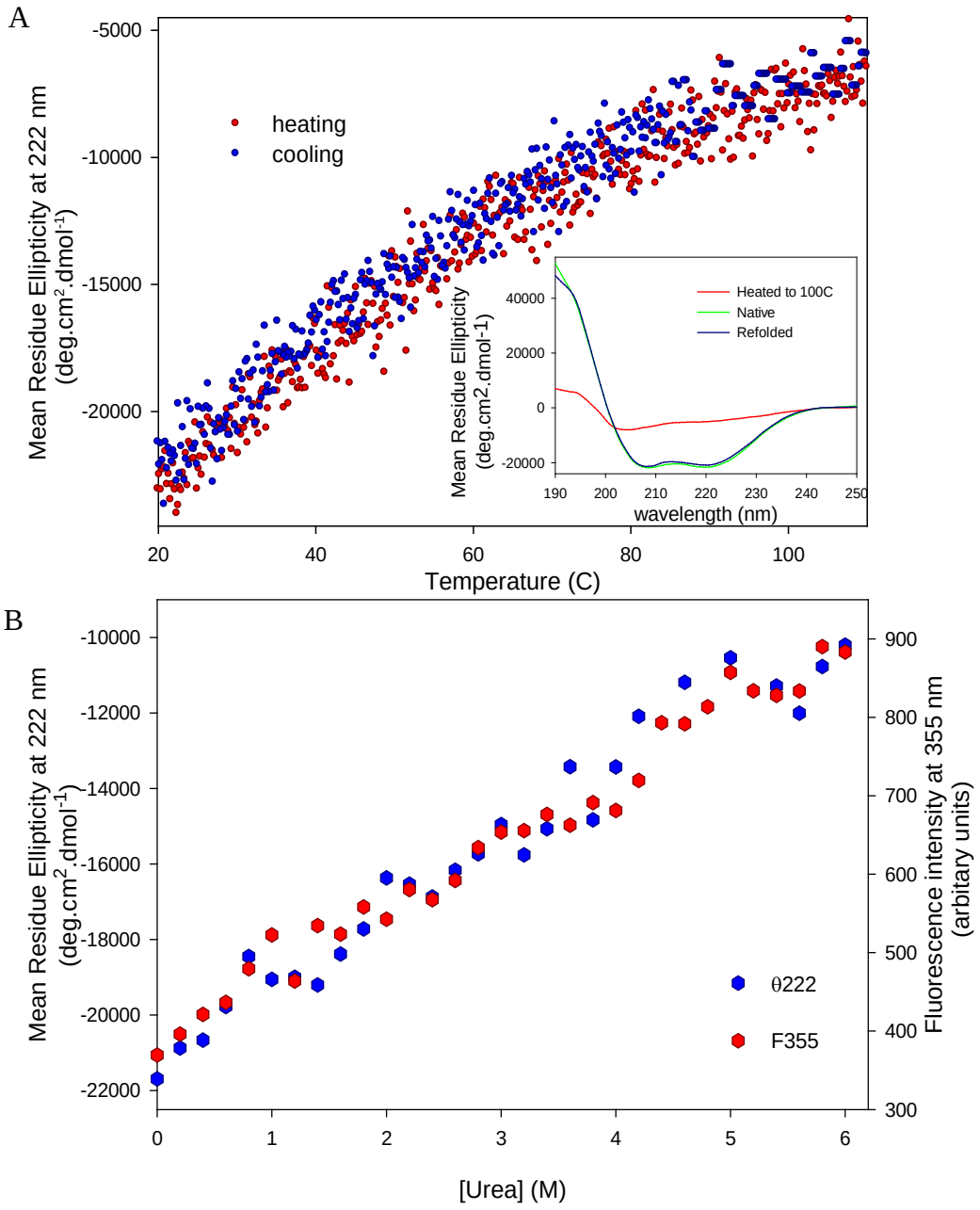


Figure 21: Unfolding of the TMR peptide in 40% TFE

(**A**) MRE at 222 nm of the TMR peptide as a function of temperature. (Insert) The TMR peptide at 20°C (green) was heated to 100°C (red) and then cooled to 20°C (blue). (**B**) MRE at 222 nm and fluorescence intensity at 355 nm of the TMR peptide as a function of urea concentration in 40% (v/v) TFE/buffer (5 mM sodium phosphate, pH 7) The unfolding of the TMR peptide is gradual and non-cooperative and does not reach a completely unfolded state. Data were plotted with Sigmaplot v. 11.0 and the spectra smoothed using the negative exponential method.

5. DISCUSSION

The crystal structure of the intergral membrane form of CLIC1 has proven difficult to acquire and thus the structure of the CLIC1 TMR in the membrane remains for the most part unexplained. Crystal structures play a significant role in understanding the folding of proteins but the scarcity of high resolution membrane protein crystal structures has led to the emergence of peptides as tools to study membrane protein folding and structure. Since the individual transmembrane segments are considered to be independently folded units in that they maintain their native fold when excised from the parent protein, peptides derived from the sequences of these membrane-embedded portions can be used to gain insight into how membrane proteins assemble to form their functional biological units in membranes (reviewed in Bordag and Keller, 2010; White *et al.*, 2001). To gather more information on the structure of the membrane-bound TMR of CLIC1, a peptide representing this region was studied in membrane mimetic systems. The effect of pH on the structure formed in these membrane-like environments as well as the stability of this structure was investigated.

5.1. Folding model of CLIC1

Understanding the structure and folding of membrane proteins is fundamental to understanding their function. The current model which has been proposed to explain how CLIC1 folds into the membrane form emphasises a structural reorganisation in the N-domain of soluble CLIC1. This domain contains the TMR consisting of a $\alpha1\beta2$ supersecondary motif in the soluble form. Upon oxidation, the N-domain undergoes a structural reorganisation into an all-helical form, with $\alpha1$ extending by two helical turns towards the C-domain (Goodchild *et al.*, 2009). In the presence of a membrane, this reorganisation exposes a hydrophobic surface that acts as a membrane docking surface in the initial step of membrane insertion (Goodchild *et al.*, 2009; Littler *et al.*, 2004). This is followed by the insertion of the N-terminal region containing the TMR across the lipid bilayer to form the transmembrane helix while the C-terminus remains in the cytosol. CLIC proteins contain a single transmembrane domain which cannot from a functional ion channel pore alone, thus a number of membrane-bound CLIC1 subunits are then thought to interact through interhelical association to form an oligomeric, functional channel (Singh, 2010). The current model for the association of CLIC1 TMR helices predicts the involvement of four protomers, each made up of 4 TMR helices (16 TMR helices) interacting to form a functional unit (as reviewed by Singh, 2010) although the nature of this association is as yet unknown. In the functional CLIC1, the positively charged

side chains of Arg29 and Lys37 would extend into the pore, forming two charged rings at the top and centre of the pore. Val33 would locate to the centre to form a hydrophobic gate, with the hydrophobic threonine residues (40 and 44) located towards the cytosolic face of the pore and playing a role in ion selectivity. This structure induction and stabilisation results from the low dielectric constant and the highly reduced number of solvent hydrogen bond donors and acceptors found in the hydrophobic core of the membrane when compared to the aqueous environment (Rath *et al.*, 2009).

This is in line with a widely accepted two-state model proposed by Popot and Engelman. In this model, self-inserting water-soluble TM sequences form an unstructured peptide that moves into the membrane interface to form an alpha-helix which then enters the membrane as the TM helix, forming independently stable alpha-helical transmembrane domains which later interact with one another to establish the proteins tertiary or quartenary structure (Jacobs and White, 1989; Popot *et al.*, 1987; Popot and Engelman, 1990; White and Wimley, 1999).

5.2. Structure of the TMR peptide

As mentioned in Section 5.1., the first step in helical membrane folding is the formation of a helical secondary structure as the hydrophobic sequence enters the membrane. The secondary structure of the TMR peptide was studied in two membrane-mimetic systems: isotropic solvent (TFE) and detergent micelles (SDS).

Conformations of the TMR peptide in both SDS and TFE were studied by CD spectroscopy. The peptide shows very little secondary structure in the absence of the membrane-mimetic systems. This structure is dramatically altered when more SDS or TFE is added, acquiring substantial helical structure. This resembles a two-state transition where one conformation is progressively depopulated in favour of another (Demchenko, 2001). There is a transition from an initially unstructured state to a helical conformation, consistent with the localisation of a peptide into a membrane in a TM conformation (Li *et al.*, 2001; MacKenzie *et al.*, 1997). This helical structure is maximal at 16 mM SDS (Figure 17). Hydrophobic domains are able to penetrate deeply into the hydrophobic core of SDS micelles and adopt an alpha-helical structure. SDS stabilises this structure mainly through hydrophobic interactions with the peptide (Han *et al.*, 1998) and relies on the hydrophobicity of the peptide rather than its helical propensity to form the helical structure (Li and Deber, 1993).

The secondary structure formed in TFE is maximal at 40% TFE with no significant increases observed at higher TFE concentrations (Figure 14). The addition of TFE enhances the inherent propensity of the TMR to form a helical structure. The dielectric constant of TFE

(~27) is similar to that of the lipid headgroup region of membrane lipids (Buck 1998, Hong *et al.*, 1999) and the hydrophobic trifluoroacetyl (CF_3) group provides a hydrophobic environment similar to that in membranes, favouring the formation of intramolecular hydrogen bonds resulting in secondary structure (Gast *et al.*, 1999). TFE induces structure by clustering preferentially around and thus limiting water access to the peptide backbone (Roccatano *et al.*, 2002). The reduced permittivity and decreased concentration of water as hydrogen bond donor and acceptor in the vicinity of the backbone when the peptide is in this membrane-mimetic system favour the formation of short-range intramolecular hydrogen bonds and subsequently secondary structure. NMR solution structures of TM domains in TFE are often not 100% helical; this is because of the poor solubility of the TM helix terminal flanks containing charged residues in lipomimetic solvents (as reviewed by Bordag and Keller, 2010). The CLIC1 TMR peptide contains 20% hydrophilic residues flanking a 10 residue hydrophobic sequence and this might account for the partial helical structure observed in TFE (~50%) (Table 1). These moderately folded structures are thought to be intermediates referred to as O-states (organic solvent-induced state). They are stable structures along the folding pathway similar to "molten globule" structures, which represent partially folded protein structures with considerable secondary structure but few if any tertiary structural contacts (Kuwajima, 1989; Ptitsyn, 1986). Organic isotropic membrane-mimetic solvents such as TFE lack the chemical and structural heterogeneity as well as the anisotropy of lipid bilayers, their increased hydrophobicity when compared with water is often the only property qualifying them as membrane-mimetic solvents and this leads to the observed O-states (reviewed by Bordag and Keller, 2010; Sundd *et al.*, 2004). Peptide environment greatly enhances peptide helicity and the movement of the TMR peptide from a largely unstructured conformation in aqueous buffer to a helical conformation in the membrane-mimetic systems suggests that the TMR peptide adopts an alpha-helical secondary structure in the membrane.

The association of peptides, whether by oligomerisation or aggregation, in membrane-mimetic systems has been studied using CD by evaluating the dependence of the peptide secondary structure on peptide concentration. TMR peptide association as a result of oligomerisation would not be observed because TFE disrupts tertiary and quartenary contacts and consequently the formation of higher order structures (Conio *et al.*, 1970; Fink and Painter, 1987; Herskovits *et al.*, 1970). In the same way that TFE excludes water as a hydrogen bond donor, TFE prevents interhelical interactions by clustering around the helix to

form solvent shells that impair such interactions (Roccatano *et al.,* 2000). The concentration-dependence study of the TMR peptide indicates that the secondary structure observed for the TMR peptide in 40% TFE is a result of monomeric TMR peptide at all peptide concentrations and not a consequence of aggregation.

5.3. Effect of pH on TMR structure

CLIC1 experiences a change of ~2 pH units as it moves from the cytoplasm to the membrane surface. This change in pH has been shown to enhance channel activity and is thought to prime the N-domain for membrane insertion (Fanucchi *et al.,* 2008; Stoychev *et al.,* 2009; Tulk *et al.,* 2002; Warton *et al.,* 2002). In order for CLIC1 to enter the membrane, the first 46 amino acids containing the TMR would need to detach from the rest of the protein and refold into a structure that can insert into the membrane. The conformational stability of the N-domain is reduced at low pH resulting in increased flexibility that would enable the structural rearrangement necessary for its insertion into the membrane (Fanucchi *et al.,* 2008; Stoychev *et al.,* 2009). In this study, the effect of pH on the structure of the TMR peptide was examined to determine whether any changes in the TMR helix structure occurred as a result of pH changes.

There was hardly any change in the observed secondary structure of the TMR in 40% TFE at different pH values. The alpha-helical structure remained comparatively similar given the negligible changes to the minima at 208 and 222 nm as the pH was changed from 5.0 to 8.0 despite the more marked incease in elllipticity between 210 nm and 220 nm throughout this pH range (Figure 19). The TMR peptide displays diminished ellipticity at pH 8.5.

To study the effect of pH on the tertiary structure of the TMR peptide, Trp35 was used as a chromophore, since its position in the centre of the TM helix would give information on any changes in the tertiary structure of the TMR peptide. If the environment of Trp35 is altered as a result of a change in pH, it is possible that the exposure of Trp35 to the surrounding solvent would be affected and this would be evident in the fluorescence of Trp35. Quenching of this fluorescence can be used to determine the accessibility of the tryptophan to the solvent. Acrylamide quenching of Trp35 in the TMR peptide helix was performed to investigate the effect of pH on the tertiary structure of the TMR peptide. The acrylamide quenching results indicate that the tertiary environment of Trp35 in the TMR helix does not experience significant change as the pH is changed (Figure 20). As mentioned, the overall charge of the

TMR peptide does not change in the range of pH 5 to 9, and thus the lack of change in the structure is understandable as none of the amino acid side chains in the TMR peptide become ionised in this range, resulting in the lack of change in the secondary structure of the TMR peptide. However, β1 in the intact CLIC1 contains amino acids with ionisable groups (Glu9 and Asp17) that would undergo protonation changes as CLIC1 moves to the membrane surface pH of ~5.5. These groups as well as others like them elsewhere in the protein would be protonated at the lower pH resulting in a change in the electrostatic interactions in the protein and would drive changes in the stability and structural characteristics of this region allowing the low permittivity and negative potential at the membrane surface to trigger the subsequent unfolding and refolding required to transform the structure into a membrane-insertable form (Fannuchi *et al.,* 2008).

5.4. Stability of the TMR peptide alpha-helical structure

TM helices in the membrane are considered to be independently stable units even when excised from their parent protein (Rath *et al.,* 2009). TM helix stability is defined as the free energy of transfer from the aqueous phase to the membrane bilayer and is determined by the sum of the transfer free energies of side chains and the helix-backbone (White and Wimley, 1999; Wimley and White, 2000; White *et al.,* 2001). TM helices in the membrane are dominated by short-range interactions among a few nearest neighbour residues making up the structure and not by long range interactions throughout the protein. Hydrogen bonding of the side chains to form the helix is an important factor in the stability of the TM helix (Creamer, 2000).

The stability of the TMR peptide was investigated using chemical (urea) and thermal denaturation. Both methods indicated a TM helix that is quite stable, unfolding gradually over a broad range of temperature and denaturant concentration (Figure 21A and B). The unfolding reaction was not co-operative. TM helix backbones undergo local and transient unfolding reactions through the sequential disruption of amide hydrogen bonds instead of a simultaneous collapse of the structure (Langosch and Arkin, 2009). TFE has been shown to increase the stability of TM peptides to denaturation resulting in helices that unfold at unusually high denaturant concentrations and temperatures (Roccatano *et al.,* 2008). When unfolded in aqueous solution, the structure of a TM peptide is less compact with higher conformational entropy, characterised by a high degree of hydration which stabilises the

unfolded form. The addition of TFE lowers the activity of water by immobilising it in the clathrate structures, making the energy of interaction for the TM peptide with water molecules costly. This results in the TM peptide adopting an entropically lower alpha-helical state that is stable in the absence of water. The added TFE stabilises the alpha-helical conformation favoured by the reduced water activity over the more hydrated unfolded state, leading to an alpha-helix that is more difficult to unfold, and thus can be considered more stable. This is a result of strengthened intramolecular hydrogen bonds, hydrophobic interactions and an enhancement of the helical propensities of the individual amino acids (Luo and Baldwin, 1997; Rohl *et al.,* 1996; Wei *et al.,* 2006). The surface tension of water is decreased upon addition of TFE (Paluch and Dynarowicz, 1984) a mechanism opposite to that of urea and other forms of denaturant which exert their effect by increasing the surface tension of water (Breslow and Guo, 1990). The TMR helix is stabilised by TFE, suggesting that this structure should also stable in the membrane.

The unfolding curves could not be fitted to a model, which requires reliable native and denatured baselines in order to calculate thermodynamic parameters such as the energy of unfolding (ΔG_u) (Santoro and Bolen, 1988).

The aim of this study was to characterise two peptides containing the TMR of CLIC1. β1-TMR which was expressed through recombinant protein overexpression could not be purified from its fusion partner and thus could not be studied further. The commercially obtained TMR peptide was characterised in 2 memebrane-mimetic systems and exhibited an alpha-helical structure that was stable to both chemical and thermal denaturation.

6. CONCLUSIONS

This study investigated employed a peptide-based approach to investigate the structure of the transmembrane region (TMR) of CLIC1 in membrane-mimetic solvents. The structure of TMR peptide becomes alpha-helical in membrane-mimetic systems and this observation is in agreement with the proposed model for CLIC1 membrane structure which predicts a transition to an alpha-helical TMR in the membrane (Goodchild *et al.*, 2009). The pH-dependence of this transition however, is due to a combination of local and global structural changes that result from the protonation changes in amino acids not contained within the TMR (Fannuchi *et al.,* 2008) and therefore no differences in the alpha-helical nature of the TMR peptide were observed at different pH. The alpha-helical conformation of the TMR would contribute to the ion conductance pore in the proposed CLIC1 homomultimeric channel (Singh, 2010). The exact nature of these channels however, could not be and was not investigated using the membrane-mimetic systems TFE and SDS micelles. These systems offer a good starting point for the study of peptide structure because of their ease of use and the broad range of permittivity values they cover. However, they are not suitable for investigating higher order structures of TM peptides and further investigations should be performed in more complex membrane model systems such as lipid bilayers (lipid veicles or bicelles) and biological membranes, using higher resolution techniques such as NMR to establish the structure of the functional CLIC1 channel pore in the membrane.

7. REFERENCES

Adamian, L. and Liang, J. (2002) Interhelical hydrogen bonds and spatial motifs in membrane proteins: polar clamps and serine zippers. Proteins 47, 209–218.

Alberts, B., Johnson, A., Lewis, J., Raff, M., Roberts, K. and Walter, P. (2002) Molecular biology of the cell (4th Ed.), pp. 560-562, 615-618, 631-633, Garland Science, New York, USA.

Arkin, I.T. and Brunger, A.T. (1998) Statistical analysis of predicted transmembrane alpha-helices. Biochim. Biophys. Acta 1429, 113-128.

Arutyunyan, A.M., Rafikova, E.R., Drachev, V.A. and Dobrov, E.N. (2001) Appearance of ‘‘beta-like’’ circular dichroism spectra on protein aggregation that is not accompanied by transition to beta-structure. Biochemistry (Mosc) 66, 1378–1380.

Ashley, R.H. (2003) Challenging accepted ion channel biology: p64 and the CLIC family of putative intracellular anion channel proteins. Mol. Membr. Biol. 20, 1-11.

Baldwin, R.L. (2003) In search of the energetic role of peptide hydrogen bonds. J. Biol. Chem. 278, 17581-17588.

Belgrader, P., Hansford, D., Kovacs, G.T.A (1999) A Minisonicator to rapidly disrupt bacterial spores for DNA analysis. Anal. Chem. 71, 4232– 4236.

Bennett, M.J., Choe, S., and Eisenberg, D. (1994) Refined structure of dimeric diphtheria toxin at 2.0 Å resolution. Protein Sci. 3, 1444-1463.

Bennion, B.J. and Daggett, V. (2003) The molecular basis for the chemical denaturation of proteins by urea. Proc. Natl. Acad. Sci. 100 (9), 5142-5147.

Berry, K.L. and Hobert, O. (2006) Mapping functional domains of chloride intracellular channel (CLIC) proteins in vivo. J. Mol. Biol. 359, 1316-1333.

Berry, K.L., Bülow, H.E., Hall, D.H. and Hobert, O. A (2003) A C..elegans CLIC-like protein required for intracellular tube formation and maintenance. Science 302, 2134-2137.

Berryman, M. and Bretsher, A. (2000) Identification of a novel member of the chloride intracellular gene family (CLIC5) that associates with the actin cytoskeleton of placental microvilli. Mol. Biol. Cell 11, 1509-1521.

Berryman, M., Bruno, J., Price, J., and Edwards, J.C. (2004) CLIC-5A functions as a chloride channel in vitro and associates with the cortical actin cytoskeleton in vitro and in vivo. J. Biol. Chem. 279, 34794-34801.

Bianchi E, Rampone R, Tealdi A, Ciferri A. (1970) The role of aliphatic alcohols on the stability of collagen and tropocollagen. J. Biol. Chem 10, 2453341–2453345.

Board, P.G., Coggan, M., Watson, S., Gage, P.W., and Dulhunty, A.F. (2004) CLIC-2 modulates cardiac ryanodine receptor Ca2+ release channels. Int. J. Biochem. Cell Biol. 36, 1599-1612.

Bocharov, E. V., Pustovalova, Y. E., Pavlov, K. V., Volynsky, P. E., Goncharuk, M. V., Ermolyuk, Y. S., Karpunin, D. V., Schulga, A. A., Kirpichnikov, M. P., Efremov, R. G., Maslen- nikov, I. V., and Arseniev, A. S. (2007) Unique dimeric structure of BNip3 transmembrane domain suggests membrane permeabi- lization as a cell death trigger. J. Biol. Chem. 282, 16256–16266.

Bordag, N. and Keller, S. (2010) Alpha-helical transmembrane peptides: a "divide and conquer" approach to membrane proteins. Chem. Phys. Lipids 163, 1-26.

Borel AC and Simon SM (1996) Biogenesis of polytopic membrane proteins: membrane segments assemble within translocation channels prior to membrane integration. Cell 85, 379-389.

Breslauer, K.J. (1995) Extracting thermodynamic data from equilibrium melting curves for oligonucleotide order-disorder transitions. Methods Enzymol. 259, 221-242.

Breslow, R. and Guo T. (1990) Surface tension measurements show that chaotropic salting-in denaturants are not just water-structure breakers. Proc. Natl. Acad. Sci. USA 87, 167-169.

Buck, M. (1998) Trifluoroethanol and colleagues: cosolvents come of age. Recent studies with peptides and proteins. Q Rev. Biophy 31, 297-355.

Call, M.E., Schnell, J.R., Xu, C., Lutz, R.A., Chou, J.J. and Wucherpfennig, K.W. (2006) The structure of the ζζ transmembrane dimer reveals polar features essential for its assembly with the T cell receptor. Cell, 127, 355-368.

Caputo, G.A. and London, E. (2003) Cumulative effects of amino acid substitutions and hydrophobic mismatch upon the transmembrane stability and conformation of hydrophobic alpha-helices. Biochemistry 42, 3275-3285.

Cartailler, J.P., .Haigler, H.T. and Luecke H. (2000) Annexin XII E105K crystal structure: identification of a pH-dependent switch for mutant hexamerization. Biochemistry 39, 2475-2483.

Chang, J.-Y.(1985) Thrombin specificity. Eur. J. Biochem. 151, 217–224.

Choe, S., Bennett, M.J., Fujii, G., Curmi, P.M., Kantardjieff, K.A., Collier, R.J. and Eisenberg, D. (1992) The crystal structure of diphtheria toxin. Nature 357, 216-222.

Choi, M.Y., Partridge, A.W., Daniels, C., Du, K., Lukacs, G.L. and Deber, C.M. (2005) Destabilization of the transmembrane domain induces misfolding in a phenotypic mutant of cystic fibrosis transmembrane conductance regulator. J. Biol. Chem. 280, 4968-4974.

Choma, C., Gratkowski, H., Lear, J. D., and DeGrado, W. F. (2000) Asparagine-mediated self-association of a model trans- membrane helix. Nat. Struct. Biol. 7, 161–166.

Chuang, J.Z., Milner, T.A., Zhu, M., and Sung, C.H. (1999) A 29 kDa intracellular chloride channel p64H1 is associated with large dense-core vesicles in rat hippocampal neurons. J. Neurosci. 19, 2919-2928.

Chung, C.T., Niemela, S.L. and Miller, R.H. (1989) One-step preparation of competent Escherichia coli: Transformation and storage of bacterial cells in the same solution. Proc. Natl. Acad. Sci. USA 86, 2172-2175.

Clore, G.M., Martin, S.R. and Gronenborn, M. (1986) Solution structure of human growth hormone releasing factor. Combined use of circular dichroism and nuclear magnetic resonance spectroscopy. J. Mol. Bio. 191, 553-561.

Cohen, S.N., Chang, A.C.Y., Boyer, H.W. and Helling, R.B. (1973) Construction of biologically functional bacterial plasmids in vitro. Proc. Natl. Acad. Sci. USA 70, 3240-3244.

Compton, L.A., Mathews, C.K. and Johnson W.C. (1987) The conformation of T4 bacteriophage dihydrofolate reductase from circular dichroism. J. Biol. Chem. 262, 13039-13043.

Conio G., Patrone E., Brighetti S. (1970) The effect of aliphatic alcohols on the helix-coil transition of poly-L-ornithine and poly-L-glutamic acid. J. Biol. Chem. 245, 3335–3340.

Creamer, T.P. (2003) Side-chain conformational entropy in protein unfolded states. Proteins 40, 443-450.

Cromer, B.A., Morton, C.J., Board, P.G., and Parker, M. (2002) From glutathione transferase to pore in a CLIC. Eur. Biophys. J. 31, 356-364.

Dawson, J.P., Weinger, J.S. and Engelman, D.M. (2002) Motifs of serine and threonine can drive association of transmembrane helices. J. Mol. Biol. 316, 799–805.

Dawson, J.P., Melnyk, R.A., Deber, C.M. and Engelman, D.M. (2003) Sequence context strongly modulates association of polar residues in transmembrane helices. J. Mol. Biol. 331, 255–262 .

Debska, G., Kicinska, A., Skalska, J. and Szewczyk A. (2001) Intracellular potassium and chloride channels: an update. Acta Biochem. Pol. 48, 137-44.

Demchenko, A. P. (2001) Concepts and misconcepts in the analysis of simple kinetics of protein folding, Curr. Protein Pept. Sci. 2, 73-98.

Do H., Falcone D., Lin J., Andrews D.W., and Johnson A.E. (1996). The cotranslational integration of membrane proteins into the phospholipid bilayer is a multistep process. Cell 85, 369-378.

Dulhunty, A., Gage, P., Curtis, S., Chelvanayagam, G., and Board, P. (2001) The glutathione transferase structural family includes a nuclear chloride channel and aryanodine receptor calcium release channel modulator. J. Biol. Chem. 276, 3319-3323.

Duncan, R.R., Westwood, P.K., Boyd, A., and Ashley, R.H. (1997) Rat brain p64H1,expression of a new member of the p64 chloride channel protein family in endoplasmic reticulum. J. Biol. Chem. 272, 23880-23886.

Dutzler, R., Campbell, E.B., Cadene, M., Chait, B.T. and MacKinnon, R.(2002) X-ray structure of a ClC chloride channel at 3.0 A reveals the molecular basis of anion selectivity. Nature 415, 287-294.

Edwards, J.C. (1999) A novel p64-related Cl channel: subcellular distribution and nephron segment-specific expression. Am. J. Physiol. 276, 398-408.

Eftink, M. R. 1991. Fluorescence quenching reactions: probing biological macromolecular structure. In Biophysical and Biochemical Aspects of Fluorescence Spectroscopy. Plenum Press, New York, NY.1–41.

Elter, A., Hartel, A., Sieben, C., Hertel, B., Fischer-Schliebs, E., Luttge, U., Moroni, A., and Thiel, G. (2007) A plant homolog of animal chloride intracellular channels (CLICs) generates an ion conductance in heterologous systems. J. Biol. Chem. 282, 8786–8792.

Fanucchi, S., Adamson, R. and Dirr, H.W. (2008) Formation of an unfolding intermediate state of soluble chloride intracellular channel protein CLIC1 at acidic pH. Biochemistry 47, 11674-11681.

Fernández-Salas, E., Sagar, M., Cheng, C., Yuspa, S. H., and Weinberg, W. C. (1999) p53 and tumor necrosis factor regulate the expression of a mitochondrial chloride channel protein. J. Biol. Chem. 274, 36488–36497.

Fernández -Salas, E., Suh, K.S., Speransky, V.V., Bowers, W.L., Levy, J.M., Adams, T., Pathak, K.R., Edwards, L.E., Hayes D.D.,Cheng, C., Steven, A.C., Weinberg, W.C., Yuspa, S.H. (2002) mtCLIC/CLIC4, an organocellular chloride channel protein is increased by DNS damage and participates in the apoptotic response to p53. Mol. Cell. Bio. 22, 3610-3620.

Fink, A.L. and Painter, B. (1987) Characterization of the unfolding of ribonuclease A in aqueous methanol solvents. Biochemistry 26, 1665-1671.

Flewelling, R.F. and Hubbell, W.L. (1986) The membrane dipole potential in a total membrane potential model. Applications to hydrophobic ion interactions with membranes. Biophys. J. 49, 541-552.

Friedli, M., Guipponi, M., Bertrand, S., Bertrand, D., Neerman-Arbez, M., Scott, H.S. and Antonarakis, S.E. (2003) Identification of a novel member of the CLIC family, CLIC6, mapping to 21q22.12. Gene 320, 31-40.

Ganesh, S. and Jayakumar R. (2002) Role of N-t-Boc group in helix initiation in a novel tetrapeptide. J. Pep. Res. 59, 249-256.

Garavito, R.M. and Ferguson-Miller, S. (2001) Detergents as tools in membrane biochemistry. J. Biol. Chem. 276, 32403–32406.

Garcia-Sáez, A.J., Mingarro, L., Pèrez-Payá, E. and Salgado, J. (2004) Membrane insertion fragments of Bcl-XL, Bax and Bid. Biochemistry 43, 10930-10943.

Gast, K., Zirwer, D., Müller-Frohne, M. and Damaschun, G. (1999) Trifluoroethanol-induced conformational transitions of proteins: insights gained from the differences between alpha-lactalbumin and ribonuclease A. Protein Sci. 8, 625-634.

Gasteiger, E., Hoogland, C., Gattiker, A., Duvaud, S., Wilkins, M.R., Appel, R.D. and Bairoch, A. (2005) Protein Identification and Analysis Tools on the ExPASy Server; (In) John M. Walker (ed): The Proteomics Protocols Handbook, Humana Press pp. 571-607.

Goodchild, S.C., Howell, M.W., Cordina, N.M., Littler, D.R., Breit S.N., Curmi, P.M.G. and Brown, L.J. (2009) Oxidation promotes insertion of the CLIC1 chloride intracellular channel into the membrane. Eur. Biophy. J. 39, 129-138.

Goodman, M. and Rosen, I.G. (1964) Conformational aspects of polypeptide structure XVI* rotatory constants cotton effects and ultraviolet absorbtion data for glutamate oligomers and co-oligomers. Biopolymers 2, 537.

Gouaux, E. (1997) Channel-forming toxins- tales of transformation. Curr. Opin. Struct. Biol. 7, 566–573.

Gratkowski, H, J D Lear, and W F DeGrado. 2001. Polar side chains drive the association of model transmembrane peptides. Proc. Nat. Acad. Sci. USA. 98, 880-885.

Han, Q., Lenz, M., Tan, Y., Xu, M., Sun, X., Tan, X.Z., Tan, X.Y., Tang, L., Miljkovic, D and Hoffman, R.M. (1998) High expression, purification and properties of recombinant homocysteine, {alpha} {gamma} -lyase. Protein. Expr. Purif. 14, 267–274.

Harrop, S.J., De Maere, M.Z., Fairlie, W.D., Rezstsova, T., Valenzuela, S.M., Mazzanti, M., Tonini, R., Qiu, M.R., Jankova, L., Warton, K., Bauskin, A.R., Wu, W.M., Pankhurst, S., Campbell, T.J., Breit, S.N., and Curmi, P.M.G. (2001) Crystal structure of a soluble form of the intracellular chloride ion channel CLIC1 (NCC27) at 1.4Å resolution. J. Biol. Chem. 276, 44993-45000.

Hennessey, J.P. and Johnson, W.C. Jr (1981) Information content in the circular dichroism of proteins. Biochemistry 20, 1058–1091.

Herskovits, T. T., Gadegbeku, B. and Jaillet, H. (1970) On the structural stability and solvent denaturation of proteins. I. Denaturation by alcohol and glycols. J. Biol. Chem. 245, 2588-2598.

Hofmann, K. and Stoffel, W. (1993) TMbase - A database of membrane spanningproteins segments. Biol. Chem. 374,166-172.

Hong, D.P., Hoshino, M., Kuboi, R., Goto, Y. (1999) Clustering of fluorine-substituted alcohols as a factor responsible for theirmarkedeffectsonproteinsandpeptides. J. Am. Chem. Soc. 121, 8427–8433.

Hunte, C. (2005) Specific protein-lipid interactions in membrane proteins. Biochem. Soc. Trans. 33, 938-942.

Imai, T., Kovalenko, A., Hirata, A. and Kidera, (2009) Molecular thermodynamics of trifluoroethanol-induced helix formation: analysis of the solvation structure and free energy by the 3D-RISM theory. Interdiscip. Sci. 1, 156-160.

Jacobs, R. E., and S. H. White. (1989) The nature of the hydrophobic binding of small peptides at the bilayer interface: implications for the insertion of transbilayer helices. Biochemistry. 28, 3421–3437.

Jelinek, R. and Kolusheva, S. (2005) Membrane interactions of host-defense peptides studied in model systems. Curr. Prot. Pep. Sci. 6, 103-114.

Jentsch, T.J., Stein, V., Weinreich, F. and Zdebik, A.A. (2001) Molecular structureand physiological function of chloride channels. Phys. Rev. 82, 503-568.

Jentsch, T.J. (1994) Molecular physiology of anion channels. Curr. Opin. Cell Biol. 6, 600–606.

Johnson, W.C. Jr (1990). Protein secondary structure and circular dichroism: a practical guide. Proteins 7, 205–214.

Jones, D.H., Ball, E.H., Sharpe, S., Barber, K.R. and Grant, C.W. (2000) Expression and membrane assembly of a transmembrane region from Neu. Biochemistry 39, 1870-1878.

Juban, M.M., Javadpour, M.M. and M D Barkley. 1997. Circular dichroism studies of secondary structure of peptides. Meth. Mol. Bio. 78, 73-78.

Kallenbach, N.R., Lyu, P., and Zhou, H. (1996) CD spectroscopy and the helix-coil transition in peptides and polypeptides. In Circular dichroism and the conformational analysis of biomolecules, (ed. G. Fasman), pp. 201–259. Plenum Press, New York.

Katragadda, M., Alderfer, J.L. and Yeagle, P.L. (2001) Assembly of a polytopic membrane protein structure from the solution structures of overlapping peptide fragments of bacteriorhodopsin. Biophys. J. 81, 1029-1036.

Kauzmann, W. (1959). Relative probabilities of isomers in cystine-containing randomly coiled polypeptides. In Sulfur in Proteins (Benesch, R., Benesch, R.E., Boyer, P., Klotz, I . , Middlebrook, W.R., Szent- Gyorgyi, A,, & Schwarz, D.R., Eds.), pp. 93-108. Academic Press, New York.

Kelly, S.M. and Price, N.C. (2009) Circular Dichroism: Studies of Proteins. In: eLS. John Wiley & Sons Ltd, Chichester.

Krishtalik, L.I. and Cramer W.A. (1995) On the physical basis for the cis-positive rule describing protein orientation in biological membranes. FEBS Lett. 369, 140- 143.

Kumaran, S. and Roy, R. (1999) Helix-enhancing propensity of fluoro and alkyl alcohols: influence of pH, temperature and cosolvent concentration on the helical conformation of peptides. J. Pep. Res. 53, 284–293.

Kuwajima, K. and Arai, M. (2000) in Mechanisms of Protein Folding, second edition (Pain, R. H., ed) pp 139-174, Oxford University Press, Great Britain.

Kyte, J. and Doolitlle, R.F. (1982) A simple method for displaying the hydropathic character of a protein. J. Mol. Biol. 157, 105-132.

Lacroix, E., Viguera AR and Serrano, L. (1998). Elucidating the folding problem of α helices: Local motifs, long-range electrostatics, ionic strength dependence and prediction of NMR parameters. J. Mol. Biol. 284, 173-191.

Lakowicz, J.R. (1983) Principles of fluorescence spectroscopy. Plenum Press, New York.

Lakowicz, J. R. (1999) Principles of fluorescence spectroscopy. Pp 11-14, 188, 237-249, 447-449. Plenum Press, New York.

Laemmli, K.U. (1970) Cleavage of structural proteins during the assembly of the head of bacteriophage T4. Nature 227, 680-685.

Landolt-Marticorena, C., Williams, K.A., Deber, C.M. and Reithmeier, R.A. (1993) Non-random distribution of amino acids in the transmembrane segments of human type I single span membrane proteins. J. Mol. Biol. 229, 602-608.

Landry, D., Sullivan, S., Nicolaides, M., Redhead, C., Edelman, A., Field, M., Al-Awqati, Q., and Edwards, J. (1993) Molecular cloning and characterisation of p64, a chloride channel protein from kidney microsomes. J. Biol. Chem. 268, 14948-14955.

Langosch, D. and Arkin, I.T. (2009) Interaction and conformational dynamics of membrane-spanning protein helices. Protein Sci., 18, 1343-1358.

Lauterwein J, Bo¨ sch C, Brown LR, Wu¨ thrich K (1979) Physico- chemical studies of the protein-lipid interactions in melittin- containing micelles. Biochim. Biophys. Acta. 556, 244–264.

Lazarova, T., Brewin K.A., Stoeber, K. and Robinson, C.R. (2004) Characterization of peptides corresponding to the seven transmembrane domains of human adenosine A2a receptor. Biochemistry 43, 12945-12954.

Lee, A.G. (2005) How lipids and proteins interact in a membrane: a molecular approach. Mol. BioSyst. 1, 203-212.

Lehrman, S.R., Tuls, J.L. and Lund, M. (1990) Peptide a-helicity in aqueous trifluoroethanol: correlations with predicted a-helicity and the secondary structure of the corresponding regions of bovine growth hormone. Biochemistry 29, 5590–5596.

Lesieur, C., Vecseysemjen, B., Abrami, L., Fivaz, M. and van der Goot, F.G. (1997) Membrane insertion - the strategies of toxins. Mol. Membr. Biol. 14, 45-46.

Li, H., Li, F., Qian, Z.M. and Sun, H. (2004) Structure and topology of the transmembrane domain 4 of the divalent metal transporter in membrane-mimetic environments. Eur. J. Biochem. 271, 1938–1951.

Li, H., Li, F., Sun, H. andQian, Z.M. (2003) Membrane-inserted conformation of transmembrane domain 4 of divalent metal transporter. Biochem. J. 372, 757–766.

Li, S.-C.and Deber, C. M. (1993) Peptide environment specifies conformation. Helicity of hydrophobic segments compared in aqueous, organic, and membrane environments. J. Biol. Chem. 268, 22795-22978.

Li,S.-C.and Deber, C. M. (1994) A measure of helical propensity for amino acids in membrane environments. Nature Struct. Biol. 1, 368–373.

Li, Y., Li, D., Zeng, Z. and Wang, D. (2006) Trimeric structure of the wild soluble chloride intracellular ion channel CLIC4 observed in crystals. Biochem. Biophys. Res. Comm. 343, 1272-1278.

Lim, B.A., Dimalanta, E.T., Potamousis, K.D., Apodaca, J., Ananthara-man, T.S. and Witkin, E.M. (1946) Inherited differences in sensitivity to radiation in Escherichia coli. Proc. Natl. Acad. Sci. USA 32, 59-68.

Littler, D.R., Harrop, S.J.,Brown, L.J., Pankhurst, G.J., Pankhurst, S., Mynott, A.V., Luciani, R. A., Mazzanti, M., Tanda, S., Berryma, M.A., Breit, S.A., Curmi, P.M.G. (2003) Comparison of vertebrate and invertebrate CLIC proteins: The crystal structures of Caenorhabditis elegans EXC-4 and Drosophila melanogaster DmCLIC. Proteins: Struct., Funct., Bioinf. 71, 364-378.

Littler, D.R., Harrop, S.J., Fairlie, D., Brown, L.J., Pankhurst, G.J., Pankhurst, S.,DeMaere, M.Z., Campbell, T.J., Bauskin, A.R., Tonini, R., Mazzanti, M., Breit, S.N. and Curmi, P.M.G. (2004) The intracellular chloride ion channel protein CLIC1 undergoes a redox-controlled structural transition. J. Biol. Chem. 279, 9298-9305.

Littler, D.R., Assaad, N.N., Harrop, S.J., Brown, L.J., Pankhurst, G.J., Luciani, P.,Aguilar, M., Mazzanti, M., Berryman, M.A., Breit, S.N. and Curmi, P.M.G. (2005)Crystal structure of the soluble form of the redox-regulated chloride ion channel protein CLIC4. FEBS J. 272, 4996-5007.

Littler, D. R., Harrop, S. J., Brown, L. J., Pankhurst, G. J., Mynott, A. V., Luciani, P., Mandyam, R. A., Mazzanti, M., Tanda, S., Berryman, M. A., Breit, S. N. and Curmi, P. M. G. (2008), Comparison of vertebrate and invertebrate CLIC proteins: The crystal structures of *Caenorhabditis elegans* EXC-4 and *Drosophila melanogaster* DmCLIC. Proteins: Struct., Funct., Bioinf. 71, 364–378.

Littler, D. R., Brown, L. J., Breit, S. N., Perrakis, A. and Curmi, P. M. G. (2010), Structure of human CLIC3 at 2 Å resolution Proteins: Struct., Funct., Bioinf. 78, 1594–1600.

Littler D.R., Harrop, S.J., Goodchild, S.C., Phang, J.M., Mynott, A.V., Jiang, L., Valenzuela, S.M., Mazzanti, M., Brown, L.J., Breit, S.N., Curmi, P.M. (2010) The enigma of the CLIC proteins: Ion channels, redox proteins, enzymes, scaffolding proteins? FEBS Lett. 584, 2093-2101.

Lottenberg, R., Christiansen, U., Jackson, C.M. and Coleman, P.L. (1891) Assay of coagulation proteases using peptide chromogenic and fluorogenic substrates. Methods Enzymol. 80, 341-361.

Luckey, M. (2008) Membrane structural biology: with biochemical and biophysical foundations. pp 1-3. Cambridge University Press, New York.

Luecke, H., Chang, B.T., Mailliard, W.S., Schlaepfer, D.D. and Haigler, H.T. (1995) Crystal structure of the annexin XII hexamer and implications for bilayer insertion. Nature. 378, 512-515.

Luo, Y, and Baldwin, R.L. (1998) Trifluoroethanol stabilizes the pH 4 folding intermediate of sperm whale apomyoglobin. JMB 279, 49-57.

MacKenzie, K.R., Prestegard, J.H. and Engelman, D.M. (1997) A transmembrane helix dimer: structure and implications. Science 276,131-133.

MacKenzie, K.R. (2006) Folding and stability of alpha-helical integral membrane proteins. Chem. Rev. 106, 1931-1977.

MacKenzie, K.R. and Fleming, K.G. (2008) Association energetics of membrane spanning alpha-helices. Struct.Bio. 18, 1-8.

Madej T, Gibrat JF, Bryant SH. (1995) Threading a database of protein cores. Proteins 23, 356-3690.

Maire, M. le, Champeil, P. and Moller, J.V. (2000) Interaction of membrane proteins and lipids with solubilizing detergents. Bioch.et Biophy. Acta 1508, 86-111.

Marion, D., Zasloff, M. and Bax, A. (1988) A two-dimensional NMR study of the antimicrobial peptide magainin 2. FEBS letters 227, 21-6.

Martin, J.L. (1995) Thioredoxin: a fold for all reasons. Structure 3, 245-250.

McMullen A.I., Marlborough D.I. and Bayley P.M. (1971) The Conformation of Alamethicin. FEBS Lett. 4, 278-280.

Menestrina, G., Forti, S., and Gambale, F. (1989) Interaction of tetanus toxin with lipid vesicles.Effects of pH, surface charge, and transmembrane potential on the kinetics of channel formation. Biophys. J. 55, 393-405.

Mi, W., Liang, Y.H., Li, L. and Su, X.D. (2008) The crystal structure of human chloride intracellular channel protein 2: a disulfide bond with functional implications. Proteins 71, 509-513.

Muchmore, S.W., Sattlen, M., Liang, H., Meadows, R.P., Harlan, J.E., Yoon, H.S., Nettesheim, D., Chang, B.S., Thompson, C.B., Wong, S.L., Ng, S.L., and Fesik, S.W. (1996) X-ray and NMR structure of human Bcl-xL, an inhibitor of programmed cell death. Nature 381, 335-341.

Muga, A., Gonzalez-Manas, J.M., Lakey, J.H., Pattus, F. and Surewicz, W.K. (1993) pH-dependent stability and membrane interaction of the pore-forming domain of colicin A. J. Biol. Chem. 268, 1553-1557.

Munoz, V. and Serrano, L. (1997) Development of the multiple sequence approximation within the agadir model of alpha-helix formayion: comparison with Zimm-Bragg and Lifson-Rolg formalisms. Biopolymers 41, 495-509.

Murzin, A. G., Brenner, S. E., Hubbard, T., Chothia, C. (1995) SCOP: a structural classification of proteins database for the investigation of sequences and structures. J. Mol. Biol. 247, 536-540.

Nishizawa, T., Nago, T., Iwatsubo, T., Forte, J.G., and Urshidani, T. (2000) Molecular cloning and characterisation of a novel chloride intracellular channelrelated protein, parchorin expressed in water secreting cells. J. Biol. Chem. 275, 11164-11173.

Pääkkönen. K., Annila, A., Sorsa, T., Pollesello, P., Tilgmann, C., Kilpeläinen, I., Karisola, P., Ulmanen, I. and Drakenberg, T. (1998) Solution structure and main chain dynamics of the regulatory domain (Residues 1–91) of human cardiac troponin C. J. Biol. Chem 273, 15633–15638.

Pace, C.N., Vajdos, F., Fee, L., Grimsley, G. and Gray, T. (1995) How to measure and predict the molar absorption coefficient of a protein. Protein Sci. 11, 2411-2423.

Pace, C., Shirley, B., McNutt, M. and Gajiwala, K., (1996) Forces contributing to the conformational stability of proteins. FASEB J. 10, 75-83.

Pace, C.N., Treviño, S., Prabhakaran, E. and Scholtz, J.M. (2004) Protein structure, stability and solubility in water and other solvents. Biol. Sci. 359, 1225-1235.

Paluch, M. and Dynarowicz, P. (1984) Electrical properties of the mixed films of 2,2,2-trifluoroethanol–ethanol at the water-air interface. J. Colloid Interface Sci. 98, 131−137.

Parker, M.W., Pattus, F., Tucker, A.D., &Tsernoglou, D. (1989).Struc- ture of the membrane-pore-forming fragment of colicin A. Nature 337, 93-96.

Parker, M.W. and Feil, S.C. (2005) Pore-forming protein toxins: from structure to function. Prog. Biophys. Mol. Biol. 88, 91-142.

Parker, M.W., Postma, J.P., Pattus, F., Tucker, A.D. and Tsernoglou, D. (1992) Refined structure of the pore-forming domain of colicin A at 2.4Å resolution. J. Mol. Biol. 224, 639-657.

Perkins, S. J. (1986) Protein volumes and hydration effects. The calculations of partial specific volumes, neutron scattering matchpoints and 280-nm absorption coefficients for proteins and glycoproteins from amino acid sequences. Eur. J. Biochem. 157, 169–180.

Phillips, S.R., Wilson, L.J. and Borkman, R.F. (1986) Acrylamide and iodide fluorescence quenching as a structural probe of tryptophan microenvironment in bovine lens crystallins, Curr. Eye Res. 5, 611–619.

Planque, M.R.R. de, Raussens, V., Contera, S.A., Rijkers, D.T.S., Liskamp, R.M.J., Ruysschaert, J.-M., Ryan, J.F., Separovic, F. and Watts, A. (2007) Beta-sheet structured beta-amyloid(1-40) perturbs phosphatidylcholine model membranes. JMB 368, 982-997.

Popa, T.V., Mant, C.T. and Hodges, R.S. (2004) Capillary electrophoresis of amphipathic alpha-helical peptide diastereomers. Electrophoresis 25, 94-107.

Popot, J. L., and Engelman, D. M. (1990) Membrane protein folding and oligomerization: The two-stage model. Biochemistry 29, 4031–4037.

Povey, J.F., Smales M.C., Hassard, S.J. and Howard, M.J. (2007) Comparison of the effects of 2,2,2-trifluoroethanol on peptide and protein structure and function. J. Struct. Bio. 157, 329-338.

Proutski, I., Karoulias, N. and Ashley, R.H. (2002) Overexpressed Chloride Intracellular Channel protein CLIC4 (p64H1) is an essential molecular component of novel plasma membrane anion channels. Biochem. Biophy. Res. Comm. 297, 317-322.

Provencher, S. W. and Glockner, L. (1981) Estimation of globular protein secondary structure from circular dichroism. Biochemistry 20, 33–37.

Ptitsyn, O.B. (1987) Protein folding: hypotheses and experiments. J Protein Chem 6, 272-293.

Qian, Z., Okuhara, D., Abe, M., and Rosner, M.R., (1999) Molecular cloning and characterization of a mitogen-activated protein kinase associated intracellular chloride channel. J. Biol. Chem. 274, 1621-1627.

Quinn, P.J. (1976) The molecular biology of cell membranes. Pp. 26-34. Macmillan Press, London, UK.

Rath, A., Tulumello, D.V. Deber, C.M. (2009) Peptide models of membrane protein folding. Biochemistry 48, 3036-3045.

Rath, A., Melnyk, R. A., and Deber, C. M. (2007) Evidence for assembly of small multidrug resistance proteins by a “two-faced” transmembrane helix. J. Biol. Chem. 281, 15546–15553.

Roccatano, D., Colombo, G., Fioroni, M. and Mark, A.E. (2002) Mechanism by which 2,2,2-trifluoroethanol/water mixtures stabilise secondary-structure formation in peptides: a molecular dynamics study. Proc. Natl. Acad. Sci. U S A. 99, 12179-12184.

Roccatano, D. (2008) Computer simulations study of biomolecules in non-aqueous or cosolvent/water mixture solutions. Curr. Protein Pept. Sci. 9, 407-426.

Rohl, C.A., Chakrabartty, A. and Baldwin, R.L. (1996) Helix propagation and N-cap propensities of the amino acids measured in alanine-based peptides in 40 volume percent trifluoroethanol. Protein Sci. 5, 2623-2637.

Roseman, M.A. (1988) Hydrophobicity of the peptide C=O...HN hydrogen- bonded group. J. Mol. Biol. 201, 621-623.

Ruan, W., Lindner, E., and Langosch, D. (2004) The interface of a membrane-spanning leucine zipper mapped by asparagine- scanning mutagenesis. Protein Sci. 13, 555–559.

Sakai, H. and Tsukihara, T. (1998) Structures of membrane proteins determined atatomic resolution. J. Biochem. (Tokyo) 124, 1051-1059.

Sal-Man, N., Gerber, D., Shai, Y., (2005) The identification of a minimal dimeriza- tion motif QXXS that enables homo- and hetero-association of transmembrane helices in vivo. J. Biol. Chem. 280 , 27449–27457.

Sambrook, J., Fritsch, E.F., and Maniatis, T. (1989) Molecular Cloning: A Laboratory Manual. Cold Spring Harbor, NY: Cold Spring Harbor Laboratory.

Santoro, M.M. and Bolen, D.W. (1988) Unfolding free energy changes determined by the linear extrapolation method. 1. Unfolding of phenylmethanesulfonyl alpha-chymotrypsin using different denaturants. Biochemistry 27, 8063–8068.

Schägger, H., von Jagow, G. (1987) Tricine-sodium dodecyl sulfate-polyacrylamide gel electrophoresis for the separation of proteins in the range from 1 to 100 kDa. Anal. Biochem. 166, 368-379.

Schägger H. (2006). Tricine–SDS-PAGE. Nature Protocols 1, 16 – 22.

Schendel, S.L., Xie, Z., Montal, M.O., Matsyama, S., Montal, M. and Reed, J.C. (1997) Channel formation by antiapoptotic protein Bcl-2. Proc. Natl. Acad. Sci. 94, 5113-5118.

Scholtz, J.M. and Baldwin, R.L. (1992) The mechanism of alpha-helix formation by peptides. Annu. Rev. Biophys. Biomol.Struct. 21, 95-118.

Senes, A., Engel, D.E., DeGrado, W.F., (2004) Folding of helical membrane proteins: the role of polar.GxxxG-like and proline motifs.Curr.Opin.Struct. Biol. 14, 465–479.

Senes, A., Ubarretxena-Belandia, I., Engelman, D.M., (2001). The C–H···O hydrogen bond: a determinant of stability and specificity in transmembrane helix interactions. Proc. Natl. Acad. Sci. U.S.A. 98, 9056–9061.

Shanks, R.A., Larocca, M.C., Berryman, M., Edwards, J.C., Urushidani, T., Navarre, J., and Goldenring, J.R. (2002) AKAP350 at the Golgi apparatus. II. Association of AKAP350 with a novel chloride intracellular channel (CLIC) family member. J. Biol. Chem. 277, 40973-40980.

Shorning, B.Y., Wilson, D.B., Meehan, R.R., Ashley, R.H. (2003) Molecular cloning and developmental expression of two chloride intracellular channel (CLIC) genes in Xenopus laevis. Dev. Genes Evol. 213, 514–518.

Singer, S.J. and Nicolson, G.L. (1972) The fluid mosaic model of the structure of cell membranes. Science 175, 720-731.

Singh, H. (2010) Two decades with dimorphic Chloride Intracellular Channels (CLICs). FEBS letters 584, 2112–2121.

Singh, H. and Ashley, R.H. (2006) Redox regulation of CLIC1 by cysteine residues associated with the putative channel pore. Biophys. J. 90, 1628-1638.

Singh, H., Ashley, R.H. (2007) CLIC4 (p64H1) and its putative transmembrane domain form poorly-selective, redox-regulated ion channels. Mol. Membr. Biol. 24, 41–52.

Singh, H., Ashley, R.H., Cousin, M.A. (2007) Functional reconstitution of mammalian chloride ion channels CLIC1, CLIC4 and CLIC5 reveals differential regulation by cytoskeletal actin. FEBS J. 274, 6306–6316.

Slupsky, C.M., Kay, C.M., Reinach, F.C., Smillie,L. B. and Sykes, B. D. (1995) Calcium-induced dimerisation of troponin C: mode of interaction and use of trifluoroethanol as a denaturant of quaternary structure. Biochemistry 34, 7365–7375.

Smith, D.B. and Johnson, K.S. (1988) Single-step purification of polypeptides expressed in Escherichia coli as fusions with glutathione S-transferase. Gene 67, 31-40.

Smith, N.W., Annunziata, O. and Dzyuba, S.V. (2009) Amphotericin B interactions with soluble oligomers of amyloid Abeta1-42 peptide. Bioorg. Med. Chem. 17, 2366-2370.

Song, L., Hobaugh, M.R., Shustak, C., Cheley, S., Bayley, H. and Gouaux, J.E. (1996) Structure of staphylococcal α-hemolysin, a heptameric transmembrane pore. Science 274, 1859–1866.

Stoychev,S. H., Nathaniel, C., Fanucchi, S., Brock, M., Li, S.,Asmus, K., Woods, V. L., Jr., and Dirr, H. W. (2009) Structural dynamics of soluble chloride intracellular channel protein CLIC1 examined by amide hydrogen-deuterium exchange mass spectrometry. Biochemistry 48, 8413–8421.

Studier, F.W.and Moffatt, B.A. (1987) 7 lysozyme inhibits transcription by T7 RNA polymerase T. Cell 49, 221-227.

Suginta, W., Karoulias, N., Aitken, A., Ashley, R.H. (2001) Chloride intracellular channel protein CLIC4 (p64H1) binds directly to brain dynamin I in a complex containing actin, tubulin and 14-3-3 isoforms. Biochem. J. 359, 55–64.

Suzuki, M., Youle, R.J., and Tjandra, N. (2000) Structure of Bax: Coregulation of dimer formation and intracellular localization. Cell 103, 645-654.

Suzuki, M., Morita, T. and Iwamoto, T. (2006) Diversity of Cl- channels.CMLS 63, 12-24.

Tamburro, A. M., Scatturin, A., Rocchi, R., Marchiori, F., Borin,. G., and Scoffone, E. (1968) Conformational-transitions of bovine pancreatic ribonuclease S-peptide, FEBS Lett. 1, 298-300.

Tanaka, S., Oda, Y., Ataka, M., Onuma, K., Fujiwara, S. and Yonezawa, Y. (2001) Denaturation and aggregation of hen egg lysozyme in aqueous ethanol solution studied by dynamic light scattering. Biopolymers 59, 370–379.

Tanford, C. (1980) The hydrophobic effect: Formation of micelles and biological membranes (2nd ed.), Wiley-Interscience.

Thuduppathy, G.R. and Hill, B. (2006) Acid destabilization of the solution conformation of Bcl-XL does not drive its pH-dependent insertion into membranes. Protein Sci. 15, 248-257.

Thuduppathy, G.R., Craig, J.W., Kholodenko, V., Schon, A. and Hill, B. (2006) Evidence that membrane insertion of the cytosolic domain of Bcl-XL is governed by an electrostatic mechanism. J. Mol. Biol. 359, 1045-5108.

Tilley, S.J. and Saibil, H. R. (2006) The mechanism of pore formation by bacterial toxins. Curr. Opin. Struct. Biol. 16, 230-236.

Tonini, R., Ferroni, A., Valenzuela, S.M., Warton, K., Campbell, T.J., Breit, S.N. and Mazzanti, M. (2000) Functional characterisation of the NCC27 nuclear protein in stable transfected CHO-K1 cells. FASEB J. 14, 1171-1178.

Tulk, B.M., and Edwards, J.C. (1998) NCC27, a homologue of intracellular chloride channel p64, is expressed in brush border of renal proximal tubule. Am. J. Physiol. 274, F1140-F1149.

Tulk, B.M., Schlesinger, P.H., Kapadia, S.A., and Edwards, J.C. (2000) CLIC-1 functions as a chloride channel when expressed and purified from bacteria. J. Biol. Chem. 275, 26986-26998.

Tulk, B.M., Kapadia, S., and Edwards, J.C. (2002) CLIC1 inserts from the aqueous phase into phospholipid membranes, where it functions as an anion channel. Am. J. Physiol. Cell Physiol. 282, C1103-C1112.

Tulumello, D.V. and Deber, C.M. (2009) SDS micelles as a membrane-mimetic environment for transmembrane segments. Biochemistry 48, 12096-120103.

Ulmschneider, M.B., Sansom, M.S.P., Di Nola, A., 2005. Properties of integral mem- brane protein structures: derivation of an implicitmembranepotential. Proteins 59, 252–265.

Ulmschneider, M.B. and Sansom, M.S.P. (2001) Amino acid distributions in integral membrane protein structures.Biochim.Biophys. Acta 1512, 1–14.

Valenzuela, S.M., Martin, D.K., Por, S.B., Robbins, J.M., Warton, K., Bootcov, M.R., Schofield, P.R., Campbell, T.J., and Breit, S.N. (1997) Molecular cloning and expression of a chloride ion channel of cell nuclei. J. Biol. Chem. 272, 12575-12582.

Valenzuela, S.M., Mazzanti, M., Tonini, R., Qui, M.R., Warton, K., Musgrove, E.A., Campbell, T.J. and Breit, S.N. (2000) The nuclear chloride ion channel NCC27 is involved in regulation of the cell cycle. J. Physiol. 529, 541-552.

Van der Goot, F.G., González-Manãs, J.M., Lakey, J.H. and Pattus, F. (1991) A ‘molten-globule’ membrane-insertion intermediate of the pore-forming domain of colicin A. Nature 354, 408-410.

Venyaminov, S.Y. and Yang, J.T. (1996) Determination of protein secondary structure. In Circular dichroism and the conformational analysis of biomolecules (ed. G. Fasman), pp. 69–107. Plenum Press, New York.

von Heijne, G., 2006. Membrane–protein topology. Nat. Rev. Mol. Cell Biol. 7, 909–918.

Warton, K., Tonini, R., Fairlie, W.D., Mathews, J.M., Valenzuela, S.M., Qiu, M.R., Wu, W.M., Pankhurst, S., Bauskin, A.R., Harrop, S.J., Campbell, T.J., Curmi, P.M.G., Breit, S.N.,

and Mazzanti, M. (2002) Recombinant CLIC1 (NCC27) assembles in lipid bilayers via a pH-dependent two-state process to form chloride ion channels with identical characteristics to those observed in Chinese hamster ovary cells expressing CLIC1. J. Biol. Chem. 277, 26003-26011.

Wei, X., Ding, S., Jiang, Y., Zeng, X.G., Zhou, H.M., 2006. Conformational changes and inactivation of bovine carbonic anhydrase II in 2,2,2-tri- Xuoroethanol solutions. Biochemistry (Mosc) 71 (Suppl. 1), S77–S82.

White, S.H. and Wimley, W.C. (1999) Membrane protein folding and stability: Physical principles, Annu. Rev. Biophys. Biomol. Struct. 28, 319-365.

White, S.H., Ladokhin, A.S., Jayasinghe, S. and Hristova, K. (2001) How membranes shape protein structure. J. Biol. Chem. 276, 32395–32398.

White, S.H., (2005) How hydrogen bonds shape membrane protein structure. Adv. Protein Chem. 72, 157–172.

Whitmore, L. and Wallace, B.A. (2004) DICHROWEB, an online server for protein secondary structure analyses from circular dichroism spectroscopic data. Nucleic Acids Res. 32, W668–W673.

Wimley, W.C. and White, S.H., 2000. Designing transmembrane α-helices that insert spontaneously. Biochemistry 39 , 4432–4442.

Wood, W.B. (1966) Host specificity of DNA produced by Escherichia coli: bacterial mutations affecting the restriction and modification of DNA. J. Mol. Biol. 16, 118–133.

Woody, R.W. (1995) Circular dichroism. Methods Enzymol. 246, 34-71.

Wu, C.S., Ikeda, K. and Yang JT (1981) Ordered conformation of polypeptides and proteins in acidic dodecyl sulfate solution. Biochemistry 20, 566–570.

Wu, C.S. and Yang, J.T. (1978) Conformation of naturally-occurring peptides in surfactant solution: its relation to the structure- forming potential of amino acid sequence. Biochem. Biophys. Res. Comm. 82, 85–91.

Xia, B., Vlamis-Gardikas, A., Holmgren, A., Write, P.E. and Dyson, J. (2001) Solution structure of Escherichia coli glutaredoxin2 shows similarity to mammalian glutathione S-transferases. J. Mol. Biol. 310, 907-918.

Xue, R., Wang, S., Qi, H., Song, Y., Wang, C., Li, F., 2008.Structure analysis of the fourth transmembrane domain of Nramp1 in model membranes. Biochim. Biophys. Acta 1778, 1444–1452.

Xue, R., Wang, S., Qi, H., Song, Y., Xiao, S., Wang, C., Li, F., 2009. Structure and topology of Slc11a1 (164-191) with G169D mutation in membrane-mimetic environments. J. Struct. Biol. 165, 27–36.

Yau, W.M., Wimley, W.C., Gawrisch, K., White, S.H., 1998. The preference of tryptophan for membrane interfaces. Biochemistry 37, 14713–14718.

Zhang, N. Chen, R., Young, N., Wishart, D., Winter, P., Weiner, J.H. and Li, L. (2007) Comparison of SDS- and methanol-assisted protein solubilization and digestion methods for Escherichia coli membrane proteome analysis by 2-D LC-MS/MS. Proteomics 7, 84-93.